Lichen, moss and peat control of C, nutrient and trace metal regime in lakes of permafrost peatlands

Liudmila Shirokova, Artem Chupakov, Irina Ivanova, Olga Moreva, Svetlana Zabelina, Nikita Shutskiy, Sergey Loiko, Oleg Pokrovsky

Lichen, moss and peat control of C, nutrient and trace metal regime in lakes of permafrost peatlands

Liudmila S. Shirokova[1,2], Artem V. Chupakov[2], Irina S. Ivanova[3], Olga Y. Moreva[2], Svetlana A. Zabelina[2], Nikita A. Shutskiy[4], Sergey V. Loiko[5], Oleg S. Pokrovsky[1]*

[1] *GET (Géosciences Environnement Toulouse) UMR 5563 CNRS; University of Toulouse, 14 Avenue Edouard Belin, 31400 Toulouse, France*

[2] *Institute of Ecological Problems of the North, Federal Center of Arctic Research, 23 Nab. Severnoi Dviny, Arkhangelsk, Russia*

[3] *Tomsk branch of the Trofimuk Institute of Petroleum Geology and Geophysics, SB RAS, Tomsk, Akademichesky 4, 634055 Tomsk, Russia*

[4] *Lomonosov Northern (Arctic) Federal University, 17, Nab. Northern Dvina, 163002, Arkhangelsk, Russia*

[5] *BIO-GEO-CLIM Laboratory, Tomsk State University, 35 Lenina, Tomsk, Russia*

*Corresponding author. Email: oleg.pokrovsky@get.omp.eu

Keywords: Organic carbon, CO_2, thermokarst, mesocosm, enclosure, vegetation, thaw pond, micronutrient

Submitted to *Science Total Environment*, after revision March 2021.

Abstract

Permafrost thaw in continental lowlands produces large number of thermokarst (thaw) lakes, which act as a major regulator of carbon (C) storage in sediments and C emission in the atmosphere. Here we studied thaw lakes of the NE European permafrost peatlands - shallow water bodies located within frozen peat bogs and receiving the majority of their water input from lateral (surface) runoff. We also conducted mesocosm experiments via interacting lake waters with frozen peat and dominant ground vegetation - lichen and moss. There was a systematic decrease in concentrations of dissolved C, CO_2, nutrients and metals with an increase in lake size, corresponding to temporal evolution of the water body and thermokarst development. We hypothesized that ground vegetation and frozen peat provide the majority of C, nutrients and inorganic solutes in the water column of these lakes, and that microbial processing of terrestrial organic matter controls the pattern of CO_2 and nutrient concentrations in thermokarst lakes. Substrate mass-normalized C, nutrient (N, P, K), major and trace metal release was maximal in moss mesocosms. After first 16 h of reaction, the pCO_2 increased ten-fold in mesocosms with moss and lichen; this increase was much less pronounced in experiments with permafrost peat. Overall, moss and lichen were the dominant factors controlling the enrichment of the lake water in organic C, nutrients, and trace metals and rising the CO_2 concentration. The global significance of obtained results is that the changes in ground vegetation, rather than mere frozen peat thawing, may exert the primary control on C, major and trace element balance in aquatic ecosystems of tundra peatlands under climate warming scenario.

1. Introduction

The surface waters of permafrost peatlands are known to exhibit strong CO_2 oversaturation with respect to atmosphere and thus, yield sizeable CO_2 emissions

(Laurion et al., 2010; Lundin et al., 2013; Roiha et al., 2015; Sepulveda-Jauregui et al., 2015; Vonk et al., 2015; Elder et al., 2018; Karlsson et al., 2021). These waters also contain high Dissolved Organic Carbon (DOC) concentrations, rendering them important reservoirs of C and related elements in Northern Hemisphere. Today, C biogeochemical cycles in C-rich peatland waters from the permafrost zone are characterized in Canadian Plane lakes (Negandhi et al., 2013; Bouchard et al., 2014; Matveev et al., 2016, 2019; Arsenault et al, 2018; Wauthy et al., 2018), small bogs of northern Sweden (Roehm et al., 2009; Hodgkins et al., 2014, 2016), and most extensively, in western Siberian lowland (WSL, Frey and Smith, 2005; Frey et al., 2007; Pokrovsky et al., 2011, 2013; Shirokova et al., 2013, 2020; Manasypov et al., 2014, 2015; Loiko et al., 2017; Serikova et al., 2019).

Among various surface waters of permafrost landscapes, recently formed thermokarst lakes are most interesting because they emit sizeable amount of CO_2 and CH_4 to the atmosphere (Walter et al., 2008; Walter-Anthony et al., 2012, 2014; Hogdkins et al., 2014; Ewing et al., 2015; Mann et al., 2015; Natali et al., 2015; Roiha et al., 2015; Schuur et al., 2015; Wik et al., 2016; Serikova et al., 2019). Further, in case of flooding or drainage, these lakes may deliver substantial amount of dissolved nutrients and metals to adjacent hydrological network (Kokelj et al., 2009; Pokrovsky et al., 2011, 2016a, b). The main interest to these shallow surface waters is in their location at the thawing permafrost front, typically in the discontinuous and isolated permafrost zone, where the soil temperature often fluctuates within the highly 'fragile' temperature range (0 to -2°C) of the permafrost (Romanovsky et al., 2010). As a result, under on-going climate warming and permafrost thaw, these waters may *i*) spread their surfaces much faster than those in the region with mineral substrates and *ii*) become highly vulnerable to water heating and heterotrophic respiration of dissolved and particulate organic matter (OM) into CO_2.

The area coverage of thaw ponds and small depressions in permafrost-affected peatlands of Northern Eurasia is not fully quantified but may range from 5 to 20% of the territory which includes Western Siberia Lowland (WSL), Northern Siberian Lowland, Kolyma and Indigirka Lowland, of overall area > 2 million km² (Polishchuk et al., 2020; Zabelina et al., 2021). In Europe, the permafrost peatlands widely occur in the NE part of it, within the Bolshezemelskaya Tundra (200,000 km²), although biogeochemical parameters of related thermokarst lakes are quite poorly known.

The main source of DOM in thaw ponds of frozen peatlands is leaching of C from allochthonous reservoirs of solid OM, such as peat and surrounding vegetation (mosses, lichens). The magnitude of this process is not yet quantified, and the relative importance of three main organic 'solid' substrates - moss, lichen and peat - in providing DOC, CO_2 and nutrients to these thaw waters is not known. This, in turn, does not allow predicting the response of these aquatic ecosystems to the change of environmental conditions such as vegetation regime and increasing the active layer thickness (ALT) and the precipitation. The latter will likely bring about a surface drainage through litter layer rather than through underlaying mineral soils. To assess the capacity of ground vegetation and peat soil to modify the chemical and gaseous regime of thaw ponds, mere observations of natural environments are not sufficient and ecosystem (mesocosm-level) manipulations are needed.

Indeed, the ecosystem manipulation or mesocosm experiments allow understanding the system behavior under various external impacts (i.e., Hering et al., 2015; de Rozari et al., 2016; Conroy et al., 2016). Although the mesocosm experiments were extensively used for boreal, permafrost- and peat-bearing aquatic landscapes (Bridgham et al., 1999; Judd and Kling, 2002; Blodau and Moore, 2003; Blodau et al., 2004; Basiliko et al., 2006; Balcarczyk et al., 2009; Green et al., 2014; Richardson et *al*., 2015; Nydahl et al., 2019), only one study (Manasypov et al., 2017) dealt with thermokarst lakes of permafrost peatlands. However, in their study, the pCO_2 and

dissolved nutrient patterns were not assessed, and two important substrates contributing to the lake water hydrochemical composition – moss and frozen peat – were not tested.

In this work, we performed mesocosm experiments on isolated water volumes of thermokarst thaw ponds and we characterized the change of chemical and gaseous (CO_2) parameters of pond water in response to the addition of peat, moss and lichen. We hypothesized that peat will be an important source of chromophoric DOM (CDOM) and nutrients, whereas a non-aromatic, bioavailable DOM and nutrients may be released from moss and lichen. To test this hypothesis, we quantified the relative capacity of various organic substrates to change the chemical composition (DOC, nutrients, metals, dissolved CO_2) of pond water over the time scale (10 to 20 days) comparable to the water residence time in small thaw ponds. Further, we characterized the hydrochemical regime of small thermokarst water bodies of poorly studied Bolshezemelskaya Tundra of NE Europe, and we quantified the C, nutrient, and trace element regime concentration change in natural ponds and lakes depending on their surface area (degree of maturity). We aimed at comparing the pattern of dissolved CO_2, DOC, nutrients and metals in natural sequence of thermokarst lake evolution to that in the mesocosm manipulation experiments in order to obtain quantitative constraints on future changes of thermokarst lake water chemical composition in response to vegetation change and frozen peat thaw. Based on obtained pattern of dissolved carbon, pCO_2 and elements, we provided first-order predictions of thermokarst lake water hydrochemistry change under various climate warming scenario.

2. Study site, experiments and analyses

2.1. Physio-geographical context of thaw ponds and thermokarst lakes of the Bolshezemelskaya Tundra

The BolsheZemelskaya Tundra (BZT) peatland is underlayed by permafrost, discontinuous on the eastern part and sporadic to isolated on the western part. The BZT is a hilly moraine lowland located between rivers Pechora and Usa (from the west and

140 south) and the Polar Ural and Pai-Khoi ridge from the east. The dominant altitudes are
141 between 100 and 150 m, created by hills and moraine ridges, composed of sands and silt
142 with boulders. Between the moraines and ridges there are many lakes, mostly of
143 thermokarst origin. The dominant soils are Histosol of peat bogs and podzol-gleys in the
144 south. The mean annual temperature is -3.1°C and the mean annual precipitation is 503
145 mm. The dominant vegetation of the tundra zone is mosses, lichens and dwarf shrubs.
146 The peat (1.0-1.5 m thick) overlays Quaternary glacial deposits over Cretaceous sands,
147 clays and silts. The dominant soil catenae are flat-mound bogs along the watershed
148 divides, which comprise the Hemic Cryic Histosols on mounds and Fibric Gelic Histosols
149 on troughs (the soil nomenclature is according to IUSS, 2014). The average thickness of
150 the active layer ranges from 145±20 cm within the depressions to 41±5 cm at the peat
151 mounds.

152 The thermokarst lakes are shallow (0.5 to 1.5 m) closed basins without distinct
153 inlet and outlets, with watershed surface area smaller or comparable to the lake water
154 area. They receive the surface inflow via lateral drainage of surrounding soil litter and
155 ground vegetation and shallow subsoil water flow over the permafrost table, which is so-
156 called suprapermafrost flow (Manasypov et al., 2015, 2017; Raudina et al., 2018). The
157 early stage of lake formation includes soil subsidences, lichen and moss submergence,
158 and peat abrasion (Audry et al., 2011; Kirpotin et al., 2011; Shirokova et al., 2013). It
159 follows by lateral spreading of shallow water bodies, when the ratio of the lake
160 circumference to the lake volume diminishes which leads to progressive decrease of
161 allochthonous (terrestrial) organic matter input to the lake.

162 The leaching of surrounding organic substrates occurs via (1) rain and melt snow
163 that provide a lateral surface input occurring over moss and lichen cover (Manasypov et
164 al., 2015), (2) direct interaction of the lake water with wave- and thermokarst-abraded
165 peat at the lake shore (Pokrovsky et al., 2011; Shirokova et al., 2013), and finally, (3)
166 suprapermafrost water interaction with frozen peat layer during water travel from

elevated points of relief to the lake, over the permafrost table (Raudina et al., 2018). Taking into account these three main processes supplying the C and inorganic solutes to the thaw lakes, in the present study, we modelled the effect of three main organic substrates – moss, lichen and frozen peat – interacting with thermokarst lake waters at controlled mesocosm conditions.

To assess natural variability of lake solutes as a function of lake size and degree of maturity, between July 14 and July 26 of 2016 and 2017, we sampled 29 stagnant isolated surface waters located within upland frozen peat bog, including depressions (permafrost subsidence), thaw ponds and thermokarst lakes (**Fig. 1 A**). Depressions in moss and lichen cover are typically filled by water from thawing of ground ice and ranged in size from 0.5 to 2 m² with an average depth between 0.1 and 0.3 m. A series of thaw ponds (10 to 1000 m² size, 0.3 to 0.5 m depth), and thermokarst lakes (10^3 to 10^6 m², 0.5 to 1.5 m depth) represented several stages of thermokarst water body maturation, from youngest small size ponds to large mature thermokarst lakes (Zabelina et al., 2021). These water bodies are similar to the sequence of thermokarst lakes and ponds described in Northern Europe (Matthews et al., 1997), Alaska (Hinkel et al., 2003) and western Siberia (Audry et al., 2011; Kirpotin et al., 2011).

The surface waters were collected from the shore (depressions) or the PVC boat (thaw ponds and thermokarst lakes). The water samples were filtered on-site using sterile single use Sartorius filters (acetate cellulose, 0.45 µm) for analyses of cations and anions. Unfiltered water samples for nutrient analyses were placed into 250-mL Milli-Q pre-cleaned PVC bottles and kept refrigerated until arrival to the laboratory, within 2-3 h after collection. Conceptual approach of field observations combined with mesocosm experiments in this study is illustrated in **Fig. 1 B**.

2.2. Mesocosm experiments

193 Closed-system mesocosms experiments were performed with thermokarst lake
194 water (pH ~ 5.5) using three organic substrates that are likely to control the
195 hydrochemistry of thermokarst lakes during ecosystem maturation. We selected a typical
196 (6760 m², depth of 1.0±0.5 m) thermokarst lake with moderate DOC (15 mg/L)
197 concentration. The lake was located in the palsa peat bog of Bolshezemelskaya Tundra,
198 40 km east of the Narian-Mar town (63º46'59" N, 75º39'08" E).

199 Peat from frozen layer of permafrost (50-70 cm from the surface which is 10 cm
200 below the maximal active layer depth), moss and lichen constituting ca. 30% and 70% of
201 peatland surface vegetation, were collected in the 100 m vicinity of thermokarst lake and
202 dried at 40°C using Osmofilm® bags during 5 days. The oligotrophic peat was 35%
203 decomposed and contained *Sphagnum angustifolium* (20%), cotton-grass *Eriophorum*
204 (25%), herbs *Scheuchzeria palustris* (15%), bog-sedge (5%), lichens (5%), dwarf shrubs
205 (5%) and some amount of wood debris (pine) and green mosses. The water was collected
206 on 15 July 2017 from the surface (0-20 cm) of the lake and immediately pre-filtered
207 through 100 µm nylon net to remove zooplankton, insects and large organic debris into
208 50-L PVC tanks. Duplicate tanks with lichen *Cladonia stellaris* (5.9 g_{dry}/L), moss
209 *Sphagnum palustris* (9.2 g_{dry}/L) and peat (20 g_{dry}/L) addition were closed with a 100 µm
210 nylon net and placed directly in the lake ensuring their vertical orientation and no
211 overflow of the lake water (**Fig. 1 A**). Additional aeration of incubated water was
212 achieved through periodic opening of the tank and gentle stirring of the content with pre-
213 cleaned plastic shovel. Control experiments included the same tanks filled with 100 µm-
214 filtered lake water without addition of organic or substrate. The wind –induced wave
215 movement in the lake provided sufficient agitation of the interior of the tank. The
216 experiment lasted 16 days. The CO_2 analyses were run each 2-3 h during first day. The
217 sampling for dissolved major and trace elements was performed after 1, 2, 4, 6, 9, 12 and
218 16 day of exposure in order to assess both short-term and long-term effect of added
219 substrate on lake water hydrochemistry.

220

221 *2.3. Chemical analyses*

222 The water temperature, pH, dissolved oxygen, and electric conductivity in natural
223 waters and mesocosm experiments were measured directly in the lake water column or
224 inside the tank using Hanna and WTW portable instruments. Dissolved CO_2
225 concentration was measured using portable submersible Vaissala Carbocap® GM70
226 Hand-held carbon dioxide meter with GMP222 probes (accuracy 1.5%). Filtered waters
227 of natural thaw ponds and lakes and of mesocosm samplings were processed using the
228 analytical approaches employed by the GET Laboratory (Toulouse) to analyze low total
229 dissolved solid (TDS), DOM-rich waters from boreal and permafrost-bearing settings
230 (Pokrovsky *et al.*, 2011, 2016 a, b; Shirokova *et al.*, 2013). The major anion
231 concentrations (Cl^- and SO_4^{2-}) were analyzed by ion chromatography (Dionex 2000i),
232 with an uncertainty of 2%. The DOC and Dissolved Inorganic Carbon (DIC) were
233 determined by a Shimadzu TOC-VSCN Analyzer with an uncertainty of 3% and a
234 detection limit of 0.1 mg/L. Specific UV absorbance (SUVA) was measured as
235 absorbance at 254 nm normalized for DOC concentration in l mg^{-1} m^{-1}). The major and
236 trace elements were measured by quadrupole ICP-MS (7500ce, Agilent Technologies).
237 Indium and rhenium were used as internal standards. The international geostandard
238 SLRS-5 (Riverine Water Reference Material for Trace Metals, certified by the National
239 Research Council of Canada) was used to check the validity and reproducibility of
240 analyses. Good agreement existed between our replicated measurements of SLRS-5 and
241 the certified values (relative difference < 15%).

242 The nutrient analyses were based on colorimetric assays (Koroleff, 1983a, b). Total
243 dissolved organic nitrogen (DON) was measured from the difference between the total
244 dissolved nitrogen (persulfate oxidation) and the total dissolved inorganic nitrogen (DIN,
245 or the sum of NH_4^+, NO_2^- and NO_3^-). Uncertainties of DON and DIN analyses were
246 between 10 and 20 % and detections limits were between 10 and 50 µg/l. Si concentration

247 was measured by spectrophotometry with molybdate blue with an uncertainty of ± 5%
248 and a detection limit of 2 µg/L.

249 The total bacterial number and dominant cell size morphology were quantified
250 using DAPI fluorescence method (Porter and Feig, 1980). In addition, we performed
251 oligotrophic and eutrophic bacteria (OB and EB, respectively) count in the course of
252 mesocosm experiments, following the standard methodology used in biodegradation
253 experiments of peat waters (i.e., Stutter et al., 2013) as also described previously
254 (Shirokova et al., 2013, 2019; Chupakova et al., 2018).

255 *2.4. Quantification of element release from organic substrates*

256 In order to calculate the dynamics of element concentration and the amount of
257 element released in the mesocosms, we normalized the difference between element
258 concentration in the experiment and the control (lake water without added substrate) to
259 the concentration of dry substrate in the mesocosm. This allowed tracing the net amount
260 of element (i, mol L^{-1}) released from the substrate (peat, moss or lichen) to the lake water
261 in the course of mesocosm experiment (Δi, mmol $kg_{dry\ substrate}^{-1}$). We estimated the
262 maximal rate (V_{max}, mmol kg^{-1} h^{-1}) of element release from substrate as a derivative of
263 average maximal change of concentration over the first 24 h. We also quantified the mean
264 rate of element release (V_{mean}) over the full duration of experiments, and the maximal
265 effect of concentration increase determined as the average of 2-3 neighboring
266 concentrations, typically after 100 h of reaction. The initial concentration used to trace
267 these dependences was the one measured 5-10 minutes following the addition of organic
268 substrate. The reason for this choice is that some elements could be present as loosely
269 bound on the surface of organic matter or within the remaining water of humid substrates,
270 notably moss and peat, and quickly released to the aqueous solution, immediately after
271 substrate addition to the reactors. The negative value of V_{max} rate was indicative of
272 element concentration decrease in the course of experiments; in such case, the rates were
273 not quantified.

3. Results

3.1. Evolution of element concentration in the natural sequence of lake growth and maturation reflected in the thermokarst lake size

The evolution of major hydrochemical parameters in the course of lake maturation (increase in size) was characterized via a Mann Kendall test of probability at 90 and 95% level of significance (**Fig. S1** of the Supplement). It is illustrated as a plot of concentration versus thaw pond and lake area for pH, pCO_2, DOC and DIC (**Fig. 2 A-D**). There was a systematic increase in pH (ca, 3 units) with lake size increase from 0.1 to 10^5 m², whereas pCO_2 and DOC concentration decreased about ten times with lake growth and maturation, when the lake size increased over 6 orders of magnitude. The lowest pH values and the highest concentrations of DOC and pCO_2 were observed at the very beginning of thermokarst activity - in small soil depressions, subsidences, water puddles and thaw ponds (< 1-10 m²). The evolution of nutrient (N, P, Si), major cation (Ca) and metal (Fe, Al) concentrations over the lake maturation was less pronounced (**Fig. 3**). The change of pH value and element (C*i*) concentration with lake area (S_{lake}) can be described by a linear function:

$$[C_i] = A \times \log S_{lake} + B \quad (1)$$

with parameters A and B of the regression listed in **Table S1**. Considering the trend of element concentration with lake size increase, two main families of solutes were distinguished (**Fig. S1**). The value of Specific Conductivity (S.C.) and concentrations of eutrophic and oligotrophic bacteria, CO_2, DOC, nutrients (NO_2, NO_3, Si, Fe), and some trace elements (Al, Co, Cd, Pb, Sb, Cs, Tl) decreased with lake size; these components formed the first group of elements. The second group of components demonstrated significant ($p < 0.05$) increase in concentration with lake size: O_2, Li, Ca, K, Y, REE, As, Hf, U and the pH value. The other elements did not show any significant ($p > 0.05$, $r <$

0.3) correlation with lake size and the probability of their concentration increase or decrease was below 90% (**Fig. S1**).

3.2. Mesocosmes of thermokarst lakes from peat palsa plateau

The addition of organic substrates to the lake water caused progressive change of concentration of most dissolved components. The maximal element yield, mean and maximal rates of DOC, nutrient, bacteria, major component (**Table 1**) and trace element (**Table S2**) release were normalized to dry weight of organic substrate and averaged across replicates. These allowed to assess the degree of substrate effect on lake water enrichment (or impoverishment) by each element. For convenience, the element concentration evolution in the mesocosms and in the control enclosures are depicted for several representative major and trace components in **Fig. S2** of the Supplement and specified by groups below.

3.2.1. Major parameters of lake water (pH, pCO_2, carbon and bacteria).

The pH of the lake water strongly decreased by ca. 1.5 units, immediately after addition of all three organic substrates (**Fig. 4 A**). The peat addition produced the lowest pH (ca. 3.75) whilst the moss and lichen addition yielded similar pH drop at the beginning of experiments; the pH then remained stable for the full duration of exposure. Specific conductivity steadily increased during experiments with mosses but did not evolve in other treatments (**Fig. 4 B**). The DIC was an order of magnitude higher in experiments with moss and lichen compared to peat and lake water control incubation (**Table 1**). The oxygen regime was similar (80-100% saturation) between lake water control and peat addition, but the O_2 level strongly decreased (ca., by a factor of 5 to 10) after first 50-100 h of experiments with moss and lichen thus producing net negative ΔO_2 values (**Fig. 4 D**).

326 The pCO_2 pattern in experimental mesocosms demonstrated a 10-fold increase
327 over the first 200 hours of lake water reaction with moss and lichen (**Fig. 4 C; Fig. S2 B**).
328 The degree of pCO_2 increase relative to the control followed the order moss > lichen >>
329 peat. However, when normalized to the amount of biomass used in mesocosm incubation,
330 the moss, lichen, and peat released 19, 34 and 4.7 mmol CO_2 kg^{-1}, respectively. The
331 DOC concentration was the highest in experiments with moss addition, rising 8 times,
332 from 20 mg/L to 160 mg/L over 2 weeks of reaction (**Fig. 4 E; S2 C**). Lichen and peat
333 addition produced similar, 2-3 fold increase in DOC over first 284 h of reaction. The
334 mass-normalized DOC yield at the end of incubation was equal to 1500, 580, and 89
335 mmol DOC kg^{-1} for moss, lichen and peat, respectively (**Table 1**).
336 The UV absorbency and $SUVA_{254}$ were drastically different among three
337 substrates and evolved different to that of DOC (**Fig. 4 F; S2 D**). Peat and moss addition
338 produced a 2-fold increase in absorbency whereas lichens did not affect the release of
339 CDOM. The SUVA decreased after 5 days of reaction with moss and lichen but remained
340 essentially constant in experiments with peat addition, when slightly positive rate
341 increase was observed.
342 The concentration of eutrophic culturable bacteria steadily increased in moss and
343 lichen mesocosms, but decreased after initial rise at 80-100 h in experiments with peat
344 additions (**Fig. S3 A**). The number of oligotrophic bacteria significantly increased with
345 time for all substrates (**Fig. S3 B**) and was ca. 1 to 2 orders of magnitude higher than that
346 in lake water control run. The mesocosms with moss and lichen addition exhibited the
347 highest concentration of cultivable bacteria. Consistent with cultivable (OB and EB)
348 bacterial numbers, the total bacterial (TB) number measured by DAPI was the highest in
349 moss and lichen treatments ((20-40)$\times 10^6$ cell mL^{-1} without systematic evolution), which
350 was sizably lower in peat treatment ((1-2)$\times 10^6$ cell mL^{-1}). The latter was comparable with
351 TB in the lake water control (5-6)$\times 10^6$ cell mL^{-1}.
352

353 3.2.3. Nutrients (Si, P, N)

354 Dissolved Si exhibited the minimal changes in the course of experiments with
355 stable concentrations achieved over the first day of reaction (**Fig. 5 A, S2 H**). The
356 biomass-normalized Si release was equal to 1.4, 0.97 and 0.26 mmol kg^{-1} for moss, lichen
357 and peat treatments (**Table 1**). Total dissolved P was dominated (> 90%) by PO_4 whose
358 yield was orders of magnitude higher in moss and lichen mesocosms compared to peat
359 addition (**Fig. 5 B**). Total dissolved N was dominated by NO_3 which was generally stable
360 from the very beginning of experiment and did not systematically evolved over 380 h of
361 exposure (**Fig. 5 C**); mosses and lichens released significant amount of nitrate, unlike
362 peat. Addition of moss yielded strong increase in NH_4^+ after 4 days of reaction however
363 the agreement between replicates was quite low (**Fig. 5 D**).

364

365 3.2.3. Major and trace elements

366 The final metal yield achieved after ~300 h of reaction for each substrate listed in
367 **Table S2** allowed distinguishing two main group of elements, depending on the moss or
368 peat control on their release in the mesocosms. Examples of major and trace elements are
369 shown in **Fig. S4**. Strong enrichment of the lake water in Li, Na, Mg, K, Fe, Cu, As, Rb,
370 Cs, Ga, Nb and Tl upon the moss addition persisted over full duration of experiments and
371 was significant ($p < 0.0001$) compared to peat and lichen treatments. Therefore, these
372 elements may serve as indicators of the dominance of moss leaching on thermokarst lake
373 water's chemistry. In contrast, high concentrations of lithogenic Be, Al, V, Ni, Y, heavy
374 REEs, Zr and Hf were observed in mesocosms with peat addition; these elements may be
375 indicative of the influence of peat on thermokarst lake water composition. Addition of
376 lichens enriched aqueous solution in Pb but removed Fe, Al, Ni, Ba, Y, Ga and Zr, as
377 supported by mean and maximal rates of element concentration increase after addition of
378 substrates (see **Table 1** and **Table S2**).

379

4. Discussion

4.1. Lake size control on C, nutrient and metal concentration in natural settings

We observed gradual decrease of S.C., pCO_2, DOC, some nutrients (Si, NO_3), and trace metals (Fe, Al Zn, Co, Cd, Pb, Cs) from small thaw depressions to thaw ponds and lakes. This is consistent with evolution of water hydrochemistry during thaw pond and thermokarst lake growth and maturation in other frozen peatlands of the world, such as WSL (Pokrovsky et al., 2011; Shirokova et al., 2013; Manasypov et al., 2014) and palsa peat bog of Canada (Peura et al., 2020). A decrease in concentrations of C, nutrients and metals with lake size may be caused by several parallel mechanisms operating at the lake shore/lake watershed and within the lake water column as depicted in **Fig. 6.** The leaching of DOC and inorganic solutes occurs from ground vegetation (mainly moss and lichen) and during peat abrasion at the lake shore (Shirokova et al., 2017; Payandi-Rolland et al., 2020a). The delivery of these substrates decreases with an increase in the ratio of lake circumference and lake watershed area to the lake volume (Manasypov et al., 2015). Non-negligible amount of C can be delivered via diffusion from lake sediments into the water column (Audry et al., 2011; Shirokova et al., 2020). An increase in the lake volume and associated decrease of solute flux lead to mere dilution of dissolved C, nutrient and metal concentration upon growth of thermokarst lake depth and area. This is reflected by a linear response of DOC concentration to the logarithm of lake water areas (**Fig. 2 C**). In addition to surface vegetation and upper (unfrozen) peat horizons, thawing of ground ice during summer period (Connoly et al., 2020; Lim et al., 2021) may provide sizeable input of DOC and related elements. It can be expected that the role of moss and lichen cover is especially pronounced for small water bodies whereas the suprapermafrost flow-delivered peat leaching products are more important for large lakes. The mineral horizons can be leached by subsoil (shallow underground) waters, especially in large lakes which exhibit deeper drainage basins and higher hydrological connectivity with subsurface reservoirs (Ala-aho et al., 2018).

407 The mechanisms that are capable removing the solutes via DOM and nutrient
408 processing within the lake water column include heterotrophic bacterial activity (Comte
409 et al., 2015; Deshpande et al., 2016; Roiha et al., 2015, 2016), photodegradation
410 (although of limited importance, Laurion et al., 2021), and photosynthesis (Tank et al.,
411 2009; Rautio et al., 2011; Przytulska et al., 2016; Bogard et al., 2019; Wauthy and
412 Rautio, 2020). Heterotrophic bacterial and photodegradation of DOM lead to coagulation
413 of Fe, Mn and trace metals and their transfer to lake sediments in the form of particulate
414 OC and metal hydroxides as it is known from laboratory (Oleinikova et al., 2017a, b) and
415 field experiments (Shirokova et al., 2019; Payandi-Rolland et al., 2020b). The second
416 mechanism is nutrient uptake by macrophytes, periphyton, and plankton, whose
417 photosynthesis brings about a pH rise and a pCO_2 decrease in large thermokarst lakes
418 compared to small thaw ponds and depressions as it is known from field observations in
419 thermokarst lakes of the Mackenzie Delta (Squires et al., 2009; Tank et al., 2009). Note
420 here that the pH increase in the course of lake maturation (**Fig. 2 A**) reflects, from the one
421 hand, the phytoplankton and periphyton photosynthetic activity (Shirokova et al., 2015).
422 From the other hand, lake size increase leads to increasing connectivity with shallow
423 ground water and subsurface waters (Manasypov et al., 2015; 2020). These waters have
424 higher pH due to their reaction with soil mineral horizons and thus can decrease the
425 overall acidity of large thermokarst lakes.
426
427 *4.2. Behavior of C, nutrient and trace metal in thermokarst lakes after moss, lichen and*
428 *peat addition in mesocosm experiments.*
429 The pattern of aqueous CO_2, DOC, nutrient and metal concentration in the presence
430 of moss, lichen and peat substrates in the mesocosm experiments can serve as an
431 experimental model of thermokarst water body evolution in the natural sequence of peat
432 thawing and lake lateral spreading. The highest pCO_2 values observed at the very
433 beginning of moss and lichen reaction with lake water (**Fig. 4 C, S2 B, Table 1**) are

consistent with elevated CO_2 measured in permafrost thaw subsidence with submerged mosses in this study (i.e., several thousand ppm, x 10 oversaturated with atmosphere, **Fig. 2 B**). High pCO_2 in small waterbodies and depressions was also reported in western Siberian (Polishchuk et al., 2018) and NE European (Zabelina et al., 2021) permafrost peatlands. Sizable CO_2 production by submerged moss and lichen may occur due to both respiration of live bryophytes, fungi and algae and heterotrophic (bacterial) degradation of DOC that was leached from moss and lichen biomass. The response of CO_2 increase to moss and lichen addition (1-2 days, **Fig. 4 C**), was much faster than the DOC increase (≥ 5 days, **Fig. 4 E**). This is also reflected in higher values of V_{mean} for CO_2 compared to DOC in the presence of both moss and lichen (**Table 1**). Such a difference suggests that the respiration of live lichen and moss rather than degradation of biomass is the main driving factor of rapid CO_2 rise. The O_2 concentration strongly decreased after first day of reaction with moss and lichen (**Fig. 4 D; S2 A**). This indicates that the heterotrophic degradation consuming O_2 from lake water was the primary cause of partially anoxic conditions in these experiments. It is worth noting that for moss and lichen, the rates of initial (0-24 h) O_2 decrease (7±1; 2.7±0.8 mmol kg^{-1}) and CO_2 increase (6±2; 4±1 mmol kg^{-1}) were comparable (**Fig. 4C**, insert). Furthermore, the heterotrophic degradation control on O_2 level in mesocosms is consistent with higher bacterial number measured in moss and lichen experiment compared to peat experiment (section 3.2.1). Therefore, results of the present study suggest that the plant-derived "fresh" DOM can be a driven factor of CO_2 rise, unlike soil refractory DOM. This is consistent with recent mesocosm experiments in a meso-eutrophic lake of the boreal zone (Nydahl et al., 2019). In these experiments, with an addition of colored allochthonous (soil) DOC, there was no relationship between bacterial activities and pCO_2.

The sphagnum moss was the most efficient substrate in terms of DOC and CO_2 production. The reason of higher reactivity of moss compared to lichen is not clear; the higher degradability of moss may be caused by its essentially wet status in natural

conditions thus allowing to initiate fast and active heterotrophic bacterial activity, necessary for an enhanced CO_2 and DOC production. In contrast, in dry lichens and frozen peat, the bacteria were rather dormant and thus not capable to efficiently degrade particulate organic matter at the time scale of mesocosm experiments. Interestingly, that at the end of experiment, corresponding to stable (steady) concentration of aqueous components, the mass-normalized effects of moss exceeded that of lichen and peat by a factor of 2 to 5 (see **Table 1** and **Table S2**). In particular, the moss mesocosm yielded the highest level of nutrients, notably PO_4^{3-}, NO_3^-, NH_4^+, K, Fe, Mn, Zn. These nutrients may be potentially limiting for aquatic plankton and periphyton of surface waters from frozen peatlands. Thus, high ammonium concentrations in surface waters derived from decomposition of vegetation are well known for wetland ecosystems (Camargo and Alvaro, 2006). We therefore suggest that, at the beginning of thermokarst development, corresponding to early stages of soil subsidences, the degradation and leaching of mosses rather than that of lichens and peat determine the evolution of C, nutrient and metal concentration in thaw waters of peatlands. In particular, high DOC and pCO_2 values at the beginning of thermokarst development, observed in the present study of NE European peatlands (**Fig. 2 B, C; S2 B, C**) and supported by other observations (Zabelina et al., 2021 and references therein) are most likely linked to moss, and in a lesser degree, to lichen degradation. Note that the presence of dense *Sphagnum* moss was reported to be the main driver of variation in DOM composition in thermokarst water bodies of the North European permafrost peatlands (Hodgkins et al., 2016).

The finding that frozen peat releases quite low amount of nutrients compared to dominant terrestrial vegetation may have a global significance. It means that in case of permafrost thaw and tundra landscape modification, the primary factor of DOC concentration and CO_2 emission flux change will be the ground vegetation regime (colonization, flooding, drying), rather than thaw of frozen peat layer and reacting of thawed peat with surface waters. Moreover, given that peat addition is not capable

488 increasing pCO_2 much higher above that of the control, it is possible that progressive
489 thawing of frozen peat and its reaction with surface fluids might not produce drastic
490 change in CO_2 emission pattern from inland waters of frozen peatlands. In contrast, the
491 regime of ground vegetation flooding and decay in these wetlands might significantly
492 increase CO_2 concentration and relevant emission fluxes at the time scale of several days
493 of reaction. The reason for this is that the response of aquatic ecosystem chemical
494 composition and CO_2 emission to the submerging of mosses is on the order of first hours
495 to first days, which is comparable with the water residence time in local depressions and
496 ephemeral puddles and ponds. This conclusion is at odds with current paradigm that
497 thawing of permafrost will greatly enhance C fluxes in aquatic system, microbial activity,
498 and CO_2 emission rate (Voigt et al., 2019, Hayes et al., 2014). In case of permafrost
499 peatlands of continental lowlands, the reactivity of frozen peat in aquatic systems will
500 have a subordinate impact on C, nutrient and metal regime in surface waters, compared to
501 lateral expansion or retreat of moss cover and flooding of moss and lichens by surface
502 waters. At the same time, the relative importance of ground vegetation in element
503 delivery to the thermokarst lakes is likely to vary depending on season. Thus, in a recent
504 study of selenium (Se) biogeochemistry in thermokarst lakes of western Siberia
505 (Pokrovsky et al., 2018), we demonstrated that, in addition to direct atmospheric fallout,
506 Se input to the lakes occurs via surface flux over moss and lichen in June (spring) and via
507 supra-permafrost flow in summer and autumn. These mechanisms are fully consistent
508 with those revealed in the present study using mesocosm approach. In particularly in
509 spring, Se, together with our trace metals of atmospheric origin, can be mobilized directly
510 from melted snow and indirectly from snow water interacting with plant litter and
511 moss/lichen biomass because the underlying peat is frozen.

512 The two groups of trace element revealed during addition of various substances to
513 the lake water (section 3.2.3) can be indicative either of moss (alkalis and alkaline-earth
514 metals, Fe, As, Cu, Ga, Nb, Tl) or peat (Be, V; Ni, Al and trivalent and tetravalent

515 hydrolysates) control on thermokarst lake water chemistry. It is not possible to ascertain
516 specific processes (leaching, adsorption, heterotrophic degradation) controlling these
517 element behavior in the mesocosm experiments without assessing the role of organic and
518 organo-mineral colloids that are likely to control element speciation in surface waters of
519 permafrost peatlands. These mechanisms may include the destabilization of Fe-organic
520 complexes, liberation of ionic Fe (III), its coagulation in the form of Fe oxyhydroxides,
521 and coprecipitation of TE with Fe hydroxides, as it happens in WSL rivers and lakes
522 (Pokrovsky et al., 2016b) and observed in experimental studies of organo-ferric colloids
523 degradation by microbial activity (Oleinikova et al., 2017b). A strong link of trivalent
524 and tetravalent hydrolysates to Fe oxy(hydr)oxides in the form of organo-ferric colloids
525 was already evidenced in the water column and porewater sediments of thermokarst lakes
526 from permafrost peatlands (Pokrovsky et al., 2011; Audry et al., 2011; Shirokova et al.,
527 2013). The elements exhibiting a concomitant release with DOC are likely to be present
528 as strongly-bound organic species. Typically, these are divalent transition metals (Me^{2+}).
529 Their organo-colloidal status is maintained in a wide range of pH and DOC
530 concentrations in thaw ponds and thermokarst lakes of western Siberia (Pokrovsky et al.,
531 2011, 2013, 2016a; Shirokova et al., 2013).
532
533 *4.3. The role of permafrost thaw and vegetation shift in hydrochemistry of thermokarst*
534 *lakes subjected to climate warming*
535 Thermokarst development in permafrost peatlands involves lateral spreading of
536 the lake without significant deepening of its basin (Polishchuk et al., 2017; Manasypov et
537 al., 2020). This leads to a decrease of the ratio water volume : border line (perimeter).
538 This was first reported for Arctic tundra by Britton (1957) and later evidenced in western
539 Siberia (Kirpotin et al., 2009, 2011; Audry et al., 2011; Manasypov et al., 2020). Such a
540 decrease yields a concomitant decrease in DOC, conductivity (major cations), Fe, Al, and
541 trace element of the lake water with an increase in the lake size (Pokrovsky et al., 2011,

542 2013; Shirokova et al., 2013; Manasypov et al., 2014, 2015). Based on results of natural
543 observation in NE Europe and mesocosm experiments, we interpret this trend as due to
544 the dominance of moss and lichen degradation at the beginning of thermokarst lake
545 formation, when small depressions in the moss/lichen cover are filled by water either
546 from thawing of soil ice or of atmospheric origin (stage 1 in **Fig. 6**). The accumulation of
547 organic and inorganic solutes in the newly-formed depressions triggers DOM, nutrient
548 and metal processing in the water column. This occurs via heterotrophic plankton
549 mineralization and sedimentation to the bottom under the dominance of allochthonous
550 input from vegetation leaching (stage 2 in **Fig. 6**). At later stages of lake development, the
551 peat becomes the main supplier of C, nutrient and metal to the water column via
552 suprapermafrost inflow as well as wave abrasion of peat at the lake shore. However,
553 relatively low reactivity of peat (i.e., Payandi-Rolland et al., 2020a and this study) does
554 not allow sufficient accumulation of organic and inorganic components in the lake water
555 column. Instead, mere dilution by atmospheric precipitation and enhanced processing of
556 autochthonous DOM and nutrients (such as photo- and biodegradation and uptake by
557 plankton and periphyton) lead to overall decrease of C, nutrient and metal concentration
558 in large lakes compared to small thaw ponds (stage 3, **Fig. 6**).

559 In this study, we hypothesized that peat is an important source of chromophoric
560 DOM (CDOM) and nutrients, whereas a non-aromatic DOM easily available by bacteria
561 may be released from mosses and lichens. As a result, the pattern of CO_2 concentration is
562 determined by a combination of nutrients and DOC delivery from solid source to aqueous
563 phase. This pattern was found to be drastically different between bryophytes (mosses),
564 symbiotic organisms (lichens) and frozen peat. This finding therefore confirms our
565 hypothesis. We further anticipated that progressive change of the ratio of lake water to
566 surrounding organic substrates in the course of lake evolution will produce a systematic
567 change in lake water chemical composition: from moss and lichen degradation control at
568 the beginning of thaw pond formation, at the stage of permafrost subsidence/depression,

569 to coastal peat abrasion and dissolution control at the later stages of lake growth and
570 maturation. At the current state of knowledge, this hypothesis cannot be unambiguously
571 verified, as it requires an estimation of vegetation cover at the small thaw ponds and
572 thermokarst lakes watershed, which is possible only with high-resolution GIS
573 approaches.

574 According to results of this study, short-term (1-10 years) consequences of
575 climate warming in permafrost peatlands will be mostly pronounced through the change
576 of ground vegetation regime. On a longer perspective (50-100 years), the increase in the
577 active layer depth (currently 1 cm y^{-1}, Johansson et al., 2011) will involve much larger
578 amount of peat in water transport within the lake watersheds. This will inevitably increase
579 the relative role of peat in element delivery from the land to the lentic waters of
580 permafrost peatlands. Furthermore, a sizable amount of highly labile C and related
581 elements can be mobilized from currently frozen peat ice into the hydrological network
582 via the suprapermafrost flow (Lim et al., 2021).

583 Overall, an increase in the active layer thickness, lake water temperature and the
584 duration of unfrozen period due to climate warming should enhance carbon and element
585 leaching from moss, lichen and peat to the thermokarst lakes. However, compared to
586 wave-induced peat abrasion at the lake border, the moss and lichen colonization,
587 submerging and degradation during permafrost thaw and subsidence formation are more
588 important drivers of thermokarst lake water's chemical composition evolution under the
589 on-going environmental changes. Note that this conclusion supports recent findings on
590 very young age of C emitted from permafrost waters which reveals that inland water
591 carbon emissions from permafrost landscapes may be more sensitive to changes in
592 contemporary carbon turnover than the release of pre-aged carbon from thawing
593 permafrost (Dean et al., 2020).

594

595 **5. Concluding remarks**

Thawing of frozen peatlands produces depressions, thaw ponds and thermokarst lakes encountered in the NE European discontinuous permafrost zone (Bolshezemelskaya Tundra). There was a systematic decrease in concentrations of dissolved OC, CO_2, nutrient and metal with an increase in the water body size. In the course of lake maturation (over six order of magnitude increase in the surface area), the pH increased by ca. 3 units while the pCO_2 and DOC concentrations decreased ten-fold. Total P, Ca, Mg increased their concentrations by a factor of 2 to 3, whereas Si, Fe, Al, NO_3 decreased concentrations with lake size increase. We interpret these changes as due to a combination of external factors (delivery of solutes from lake watershed) and DOM, nutrient and metal processing in the water column.

Mesocosm experiments on thermokarst lake water in the presence of frozen peat, moss and lichen demonstrated that moss and lichen leaching and degradation, rather than peat abrasion, act as a main driver of thermokarst lake water's evolution. The mass-normalized release of DOC, macro nutrients (Si, N, P), major elements (K, Na, Ca, Mg), micronutrients and trace metals (Fe, Mn, Cu, As, Rb, Cs, Tl) was controlled essentially by moss and, in a lesser degree, lichen with almost negligible impact of peat. When comparing to natural sequence of lakes and ponds chemical composition, these mesocosm experiments allowed to characterize the water chemistry during the first step of thaw pond formation, when the moss leaching determines the hydrochemical features of surface water. Upon progressive increase in the lake size, the lichen and moss leaching at the watershed surface become less important than the delivery of peat leaching products by the suprapermafrost flow. This happens due to an increase in the ratio of lake circumference to the lake volume which decreased the delivery of external terrestrial (allochthonous) material. In contrast, when lake water volume increases, the relative role of autochthonous processes of DOM, nutrient and metal transformation, such as photo- and bio-degradation, and phytoplankton/periphyton activity also increase. This leads to

622 gradual removal of DOC, nutrients and metals due to C emission to atmosphere and
623 element deposition to the lake bottom.

624 Because moss leaching is likely to be most important process controlling
625 hydrochemistry of dissolved elements and CO_2 emission/burial pattern in thermokarst
626 water bodies, the response of the moss coverage regime to permafrost thaw and climate
627 warming in NE European frozen peatlands will chiefly define the DOC and nutrient
628 cycling in lentic waters and CO_2 emission fluxes. Given that the vegetation biomass
629 leaching reactions are very fast, on the order of first hours to days, the hydrological
630 pattern of moss and lichen flooding rather than biogeochemical reactions within the peat
631 soil profile will be controlling short-term response of peat palsa landscapes to permafrost
632 thaw and temperature rise. This contrasts a dominant view that thawing of frozen peat
633 provides the main contribution to the negative feedback of environmental response to the
634 climate change. At least on a short-term scale, the peat thaw may be a subordinate factor
635 of biogeochemical C fluxes compared to the change of wetting and flooding regime of the
636 lake shoreline and moss persistence/growth on the tundra surface.

637

638 **Acknowledgements:**

639 We acknowledge the main support from a RFBR grants 19-55-15002, and 20-05-00729_a
640 and RSF grant No 18-77-10045 for data analysis. Partial support from Belmont Forum
641 project VULCARE is also acknowledged.
642
643
644

645 **References**

646 Ala-Aho, P., Soulsby, C., Pokrovsky, O.S., Kirpotin, S.N., Karlsson, J., et al., 2018.
647 Using stable isotopes to assess surface water source dynamics and hydrological
648 connectivity in a high-latitude wetland and permafrost influenced landscape. J.
649 Hydrology 556, 279–293.
650 Arsenault, J., Talbot, J., Moore, T.R., 2018. Environmental controls of C, N and P
651 biogeochemistry in peatland ponds. Sci. Total Environ. 631-632, 714-722.
652 Audry, S., Pokrovsky, O.S., Shirokova, L.S., Kirpotin, S.N., Dupré, B., 2011. Organic
653 matter mineralization and trace element post-depositional redistribution in
654 Western Siberia thermokarst lake sediments. Biogeosciences 8, 3341–3358.
655 http://dx.doi.org/10.5194/bg-8-3341-2011.
656 Balcarczyk, K.L., Jones, J.B., Jaffé, R., Maie, N., 2009. Stream dissolved organic matter
657 bioavailability and composition in watersheds underlain with discontinuous

permafrost. Biogeochemistry 94, 255–270. http://dx.doi.org/10.1007/s10533-009-9324-x.
Basiliko, N., Moore, T.R., Jeannotte, R., Bubier, J.L., 2006. Nutrient input and carbon and microbial dynamics in an ombrotrophic bog. Geomicrobiol. J. 23, 531–543. DOI: 10.1080/01490450600897278.
Blodau, C., Moore, T., 2003. Experimental response of peatland carbon dynamics to a water table fluctuation. Aquat. Sci. 65, 47–62. http://dx.doi.org/10.1007/s000270300004.
Blodau, C., Basiliko, N., Moore, T.R., 2004. Carbon turnover in peatland mesocosms exposed to different water table levels. Biogeochemistry 67, 331–351. http://dx.doi.org/10.1023/B:BIOG.0000015788.30164.e2.
Bogard, M.J., Kuhn, C.D., Johnston, S.E., Striegl, R.C., Holtgrieve, G.W. et al., 2019. Negligible cycling of terrestrial carbon in many lakes of the arid circumpolar landscape. Nature Geoscience 12, 180-185.
Bouchard, F., Francus, P., Pienitz, R., Laurion, I., Feyte, S., 2014. Subarctic thermokarst ponds: Investigating recent landscape evolution and sediment dynamics in thawed permafrost of Northern Québec (Canada). Arct. Antarct. Alp. Res. 46 (1) 251-271., DOI : 10.1657/1938-4246-46.1.251
Bridgham, D.S., Pastor, J., Updegraff, K., Malterer, J.T., Johnson, K., Harth, C., Chen, J., 1999. Ecosystem control over temperature and energy flux in northern peatlands. Ecol. Appl. 9, 1345–1358.
Britton, M.E., 1957. Vegetation of the Arctic Tundra, in: Hanson, H.P. (Ed.), Arctic biology (18th Annual Biology Colloquium). Corvalis, Ore., Oregon State College, pp. 26–61.
Camargo, J., Alvaro A., 2006. Ecological and toxicological effects of inorganic nitrogen pollution in aquatic systems: A global assessment. Environment Internat. 32, 831-849.
Chupakova, A. A., Chupakov, A. V., Neverova, N. V., Shirokova, L. S., and Pokrovsky, O. S., 2018. Photodegradation of river dissolved organic matter and trace metals in the largest European Arctic estuary. Sci. Total Environ. 622–623, 1343–1352.
Comte J., Monier A., Crevecoeur S., Lovejoy C., Vincent W.F., 2015. Microbial biogeography of permafrost thaw ponds across the changing northern landscape. Ecography 28, 1-10. doi: 10.1111/ecog.01667.
Connolly, C.T., Cardenas, M.B., Burkart, G.A., Spencer, R.G.M., McClelland, J.W., 2020. Groundwater as a major source of dissolved organic matter to Arctic coastal waters. Nat. Commun. 11, 1–8. https://doi.org/10.1038/s41467-020-15250-8
Conroy, E., Turner, J.N., Rymszewicz, A., Bruen, M., O'Sullivan, J.J., Lawler, D.M., Lally, H., Kelly-Quinn, M., 2016. Evaluating the relationship between biotic and sediment metrics using mesocosms and field studies. Sci. Total. Environ. 568, 1092–1101. http://dx.doi.org/10.1016/j.scitotenv.2016.06.168.
de Rozari, P., Greenway, M., El Hanandeh, A., 2016. Phosphorus removal from secondary sewage and septage using sand media amended with biochar in constructed wetland mesocosms. Sci. Total Environ. 569–570, 123–133. http://dx.doi.org/10.1016/j.scitotenv.2016.06.096.
Dean, J. F., Meisel, O. H., Martyn Rosco, M., Marchesini, L.B., Garnett, M.H., Lenderink, H., … Dolman, A.J., 2020. East Siberian Arctic inland waters emit mostly contemporary carbon. Nature Comm. 11(1), doi:10.1038/s41467-020-15511-6.
Deshpande, B. N., Crevecoeur, S., Matveev, A., and Vincent, W. F., 2016. Bacterial production in subarctic peatland lakes enriched by thawing permafrost, Biogeosciences 13, 4411-4427.
Elder, C.D., Xu, X., Walker, J., Schnell, J.L. et al., 2018. Greenhouse gas emissions from diverse Arctic Alaskan lakes are dominated by young carbon. Nat. Clim. Chang. 8,

166-171.
Ewing, S.A., O'Donnell, J.A., Aiken, G.R., Butler, K., Butman, D., Windham-Myers, L., Kanevsiy, M.Z., 2015. Long-term anoxia and release of ancient, labile carbon upon thaw of Pleistocene permafrost. Geophys. Research. Lett. 42, 10730–10738. http://dx.doi.org/10.1002/2015GL066296.
Frey, K.E., Siegel, D.I., Smith, L.C., 2007. Geochemistry of west Siberian streams and their potential response to permafrost degradation. Water Res. Research 43, W03406. http://dx.doi.org/10.1029/2006WR004902.
Frey, K.E., Smith, L.C., 2005. Amplified carbon release from vast West Siberian peatlands by 2100. Geophys. Res. Lett. 32, L09401. http://dx.doi.org/10.1029/2004GL022025.
Green, S.M., Baird, A.J., Boardman, C.P., Gauci, V., 2014. A mesocosm study of the effect of restoration on methane (CH_4) emissions from blanket peat. Wetl. Ecol. Manag. 22, 523–537. http://dx.doi.org/10.1007/s11273-014-9349-3.
Hayes, D.J., Kicklighter, D.W., McGuire A.D., Chen, M., Zhuang, Q., Yuan, F., Melillo, J.M., Wullschleger, S.D., 2014. The impacts of recent permafrost thaw on land–atmosphere greenhouse gas exchange. Environ. Res. Lett. 9, 045005 doi:10.1088/1748-9326/9/4/045005.
Hering, D., Carvalho, L., Argillier, C., Beklioglu, M., Borja, A., Cardosof, A.C., Duelg, H., Ferreirah, T., Globevniki, L., Hanganuj, J., Hellstenk, S., Jeppesenl, E., Kodešm, V., Solheimn, A.L., Nõgeso, T., Ormerodp, S., Panagopoulosq, Y., Schmutzr, S., Venohrs, M., Birka, S., 2015. Managing aquatic ecosystems and water resources under multiple stress — An introduction to the MARS project. Sci. Total Environ. 503–504, 10–21.
Hinkel, K.M., Eisner, W.R., Bockheim, J.G., Nelson, F.E., Peterson, K.M., Dai, X., 2003. Spatial extent, age, and carbon stocks in drained thaw lake basins on the Barrow Peninsula, Alaska. Arct. Antarct. Alp. Res. 35: 291–300
Hodgkins, S.B., Tfaily, M.M., McCalley, C.K., Logan, T.A., Crill, P.M., Saleska, S.R., Rich, V.I., Chanton, J.P., 2014. Changes in peat chemistry associated with permafrost thaw increase greenhouse gas production. PNAS 111, 5819–5824. http://dx.doi.org/10.1073/pnas.1314641111.
Hodgkins, S.B., Tfaily, M.M., Podgorski, D.C., McCalley, C.K., Saleska, S.R… Cooper, W.T., 2016. Elemental composition and optical properties reveal changes in dissolved organic matter along a permafrost thaw chronosequence in a subarctic peatland. Geochim. Cosmochim. Acta 187, 123-140.
IUSS Working Group WRB, 2014. World Reference Base for Soil Resources 2014. International soil classification system for naming soils and creating legends for soil maps. World Soil Resources Reports No. 106. FAO, Rome
Johansson, M., Åkerman, J., Keuper, F., Christensen, T.R., Lantuit, H., Callaghan, T. V., 2011. Past and present permafrost temperatures in the Abisko area: Redrilling of boreholes. Ambio 40, 558–565. https://doi.org/10.1007/s13280-011-0163-3
Judd, K.E., Kling, G.W., 2002. Production and export of dissolved C in arctic tundra mesocosms: the roles of vegetation and water flow. Biogeochemistry 60, 213–234. http://dx.doi.org/10.1023/A:1020371412061.
Karlsson, J., Serikova, S., Rocher-Ros G., Denfeld B., Vorobyev S.N., Pokrovsky O.S., 2021. Carbon emission from Western Siberian inland waters. Nature Communication 12, 825. https://doi.org/10.1038/s41467-021-21054-1.
Kirpotin, S., Berezin, A., Bazanov, V., Polishchuk, Yu., Vorobiov, S., Mironycheva-Tokoreva, N., Kosykh, N., Volkova, I., Dupre, B., Pokrovsky, O., Kouraev, A., Zakharova, E., Shirokova, L., Mognard, N., Biancamaria, S., Viers, J., Kolmakova, M., 2009. Western Siberia wetlands as indicator and regulator of climate change on the global scale. Int. J. Environ. Stud. 66, 409–421. http://dx.doi.org/10.1080/00207230902753056.

765 Kirpotin, S., Polishchuk, Y., Bryksina, N., Sugaipova, A., Kouraev, A., Zakharova, E.,
766 Pokrovsky, O.S., Shirokova, L.S., Kolmakova, M., Manassypov, R., Dupre, B.,
767 2011. West Siberian palsa peatlands: Distribution, typology, cyclic development,
768 present day climate-driven changes, seasonal hydrology and impact on CO_2
769 cycle. Int. J. Environ. Stud. 68, 603–623.
770 http://dx.doi.org/10.1080/00207233.2011.593901.
771 Kokelj, S.V., Zajdlik, B., Thompson, M.S., 2009. The impacts of thawing permafrost on
772 the chemistry of lakes across the subarctic boreal-tundra transition, Mackenzie
773 Delta region, Canada. Permafrost Periglac. Proc. 20, 185–199.
774 http://dx.doi.org/10.1002/ppp.641.
775 Koroleff, F., 1983a. Total and organic nitrogen. In: Grasshoff K., Ehrhardt M. &
776 Kremling K. (eds.), Methods for Seawater Analysis, Verlag Chemie Weinheim,
777 pp. 162–168.
778 Koroleff, F., 1983b. Determination of phosphorus. In: Grasshoff, K., Ehrhardt, M.,
779 Kremling, K. (eds.), Methods for Seawater Analysis. Verlag Chemie Weinheim,
780 pp. 125–136.
781 Laurion, I., Vincent, W.F., MacIntyre, S., Retamal, L., Dupont, C., Francus, P., Pienitz,
782 R., 2010. Variability in greenhouse gas emissions from permafrost thaw ponds.
783 Limnol. Oceanogr. 55, 115–133. http://dx.doi.org/10.4319/lo.2010.55.1.0115.
784 Laurion, I., Massicotte, P., Mazoyer, F., Negandhi, K., Mladenov, N., 2021. Weak
785 mineralization despite strong processing of dissolved organic matter in Eastern
786 Arctic tundra ponds. Limnol. Oceanogr. 66 (S1), S47-S63. doi:
787 10.1002/lno.11634.
788 Lim, A.G., Loiko, S.V., Kuzmina, D., Krickov, I.V., Shirokova, L.S., Kulizhsky, S.P.,
789 Vorobyev, S.N., Pokrovsky, O.S., 2021. Dispersed ground ice of permafrost
790 peatlands: a non-accounted for source of C, nutrients and metals. Chemosphere
791 226, Art No 128953. https://doi.org/10.1016/j.chemosphere.2020.128953.
792 Loiko, S.V., Pokrovsky, O.S., Raudina, T., Lim, A., Kolesnichenko, L.G., Shirokova,
793 L.S., Vorobyev, S.N., Kirpotin, S.N., 2017. Abrupt permafrost collapse enhances
794 organic carbon, CO2, nutrient, and metal release into surface waters. Chemical
795 Geol. 471, 153–165.
796 Lundin, E. J., Giesler, R., Persson, A., Thompson, M. S. & Karlsson, J. Integrating
797 carbon emissions from lakes and streams in a subarctic catchment. J. Geophys.
798 Res. Biogeosciences 118, 1200–1207 (2013).
799 Manasypov, R.M., Pokrovsky, O.S., Kirpotin, S.N., Shirokova, L.S., 2014. Thermokarst
800 lake waters across the permafrost zones of western Siberia. The Cryosphere 8,
801 1177–1193. http://dx.doi.org/10.5194/tc-8-1177-2014.
802 Manasypov, R.M., Vorobyev, S.N., Loiko, S.V., Kritzkov, I.V., Shirokova, L.S.,
803 Shevchenko, V.P., Kirpotin, S.N., Kulizhsky, S.P., Kolesnichenko, L.G.,
804 Zemtzov, V.A., Sinkinov, V.V., Pokrovsky, O.S., 2015. Seasonal dynamics of
805 organic carbon and metals in thermokarst lakes from the discontinuous
806 permafrost zone of western Siberia. Biogeosciences 12, 3009–3028.
807 http://dx.doi.org/10.5194/bg-12-3009-2015.
808 Manasypov, R.M., Shirokova, L.S., Pokrovsky, O.S., 2017. Experimental modeling of
809 thaw lake water evolution in discontinuous permafrost zone: role of peat and
810 lichen leaching and ground fire. Science Total Environ. 580, 245-257.
811 Manasypov, R.M., Lim, A.G., Krickov, I.V., Shirokova, L.S., Vorobyev, S.N.,
812 Pokrovsky, O.S., 2020. Spatial and seasonal variability of C, nutrient and trace
813 metal concentration in thermokarst lakes of western Siberia across a permafrost
814 gradient. Water, 12, Art No 1830; doi:10.3390/w12061830.
815 Mann, P.J., Eglinton, T.I., Mcintyre, C.P., Zimov, N., Davydova, A., Vonk, J.E., Holmes,
816 R.M., Spencer, R.G.M., 2015. Utilization of ancient permafrost carbon in
817 headwaters of Arctic fluvial networks. Nat. Commun. 6, 7856.
818 http://dx.doi.org/10.1038/ncomms8856.

819 Matthews, J. A., Dahl, S.-O., Berrisford, M.S., Nesje, A., 1997. Cyclic development and
820 thermokarstic degradation of palsas in the mid-alpine zone at Leirpullan,
821 Dovrefjell, Southern Norway. Permafr. Periglac. Process. 8, 107–122.
822 Matveev, A., Laurion, I., Deshpande, B.N., Bhiry, N., Vincent, W.F., 2016. High
823 methane emissions from thermokarst lakes in subarctic peatlands. Limnol.
824 Oceanogr. 61 (S1), S150-S164.
825 Matveev, A., Laurion, I., Warwick, V.F., 2019. Winter accumulation of methane and its
826 variable timing of release from thermokarst lakes in subarctic peatlands. J.
827 Geophys. Res. - Biogeosciences 124(11), 3521-3535.
828 Natali, S.M., Schuur, Ea.G., Mauritz, M., Schade, J.D., Celis, G., Crummer, K.G.,
829 Johnston, C., Krapek, J., Pegoraro, E., Salmon, V.G., Webb, E.E., 2015.
830 Permafrost thaw and soil moisture driving CO_2 and CH_4 release from upland
831 tundra. J. Geophys. Res.-Biogeo. 120, 525–537.
832 http://dx.doi.org/10.1002/2014JG002872.
833 Negandhi, K., Laurion, I., Whiticar, M. J., Galand, P. E., Xu, X. Lovejoy, C., 2013. Small
834 thaw ponds: An unaccounted source of methane in the Canadian high Arctic.
835 PLoS ONE, 8 (11) : e78204.
836 Nydahl, A.C., Wallin M.B., Tranvik, L.J., Hiller, C., Attermeyer, K., Julie A. Garrison,
837 J.A., Chaguaceda, F., Scharnweber, K., Weyhenmeyer, G.A., 2019. Colored
838 organic matter increases CO_2 in meso-eutrophic lake water through altered light
839 climate and acidity. Limnol. Oceanogr. 64(2), 744-756, DOI:
840 10.1002/lno.11072.
841 Oleinikova, O.V., Drozdova, O.Y., Lapitskiy, S.A., Demin, V.V., Bychkov, A.Y.,
842 Pokrovsky, O.S., 2017a. Dissolved organic matter degradation by sunlight
843 coagulates organo-mineral colloids and produces low-molecular weight fraction
844 of metals in boreal humic waters. Geochim. Cosmochim. Acta 211, 97–114.
845 Oleinikova, O., Shirokova, L.S., Gerard, E., Drozdova, O.Yu., Lapitsky, S.A., Bychkov,
846 A.Y., Pokrovsky; O.S., 2017b. Transformation of organo-ferric peat colloids by
847 a heterotrophic bacterium. Geochim. Cosmochim. Acta 205, 313–330.
848 Payandi-Rolland, D., Shirokova, L.S., Nakhle, P., Tesfa, M., Abdou, A., Causserand, C.,
849 Lartiges, B., Rols, J.-L., Guérin, F., Bénézeth, P., Pokrovsky, O.S., 2020a.
850 Aerobic release and biodegradation of dissolved organic matter from frozen
851 peat: Effects of temperature and heterotrophic bacteria. Chem. Geol. 536,
852 119448. https://doi.org/10.1016/j.chemgeo.2019.119448.
853 Payandi-Rolland, D., Shirokova, L.S., Tesfa, M., Lim, A.G., Kuzmina, D., Benezeth, P.,
854 Karlsson, J., Giesler, R., Pokrovsky, O.S., 2020b. Dissolved organic matter
855 biodegradation along a hydrological continuum in a discontinuous permafrost
856 area: case study of Northern Siberia and Sweden. Science Total Environ. 749,
857 Art No 141463.
858 Peura, S., Wauthy, M., Simone, D., Eiler, A., Einarsdottir, K., Rautio, M., Bertilsson, S.,
859 2020. Ontogenic succession of thermokarst thaw ponds is linked to dissolved
860 organic matter quality and microbial degradation potential. Limnol. Oceanogr.
861 65, S248-S263.
862 Pokrovsky, O.S., Shirokova, L.S., Kirpotin, S.N., Audry, S., Viers, J., Dupré, B., 2011.
863 Effect of permafrost thawing on organic carbon and trace element colloidal
864 speciation in the thermokarst lakes of western Siberia. Biogeosciences. 8, 565–
865 583. http://dx.doi.org/10.5194/bg-8-565-2011.
866 Pokrovsky, O.S., Shirokova, L.S., Kirpotin, S.N., Kulizhsky, S.P., Vorobiev, S.N., 2013.
867 Impact of Western Siberia heat wave 2012 on greenhouse gases and trace metal
868 concentration in thaw lakes of discontinuous permafrost zone. Biogeosciences
869 10, 5349–5365. http://dx.doi.org/10.5194/bg-10-5349-2013.
870 Pokrovsky, O.S., Manasypov, R.M., Loiko, S., Krickov, I.A., Kopysov, S.G.,
871 Kolesnichenko, L.G., Vorobyev, S.N., Kirpotin, S.N., 2016a. Trace element

transport in western Siberia rivers across a permafrost gradient. Biogeosciences 13, 1877–1900. http://dx.doi.org/10.5194/bg-13-1877-2016.

Pokrovsky, O.S., Manasypov, R.M., Loiko, S.V., Shirokova, L.S., 2016b. Organic and organo-mineral colloids of discontinuous permafrost zone. Geochim. Cosmochim. Acta 188, 1–20. http://dx.doi.org/10.1016/j.gca.2016.05.035.

Polishchuk, Y. M., I. N. Muratov, and V. Y. Polishchuk. 2020. Remote research of spatiotemporal dynamics of thermokarst lakes fields in Siberian permafrost. In: O.S. Pokrovsky, S. N. Kirpotin, A. I. Malov [eds], (2020) The Arctic: Current Issues and Challenges. Nova Publ., Inc. New York, 425 pp, ISBN: 978-1-53617-306-2.

Polishchuk, Y.M., Bogdanov, A.N., Muratov, I.N., Polishchuk, V.Y., Lim, A., Manasypov, R.M., Shirokova, L.S., Pokrovsky, O.S., 2018. Minor contribution of small thaw ponds to the pools of carbon and methane in the inland waters of the permafrost-affected part of the Western Siberian Lowland. Environ. Res. Lett. 13, 04500. https://doi.org/10.1088/1748-9326/aab046.

Polishchuk, Y.M., Bogdanov, A.N., Polischuk, V.Y., Manasypov, R.M., Shirokova, L.S., Kirpotin, S.N., Pokrovsky, O.S., 2017. Size-distribution, surface coverage, water, carbon and metal storage of thermokarst lakes (> 0.5 ha) in permafrost zone of the Western Siberia Lowland. Water 9, 228, doi:10.3390/w9030228.

Raudina, T.V., Loiko, S.V., Lim, A., Manasypov, R.M., Shirokova, L.S., Istigechev, G.I., Kuzmina, D.M., Kulizhsky, S.P., Vorobyev, S.N., Pokrovsky, O.S., 2018. Permafrost thaw and climate warming may decrease the CO_2, carbon, and metal concentration in peat soil waters of the Western Siberia Lowland. Sci. Total Environ. 634, 1004–1023. https://doi.org/10.1016/j.scitotenv.2018.04.059

Porter, K. G., and Feig, Y. S., 1980. The use of DAPI for identifying and counting aquatic microflora, Limnol. Oceanogr. 25, 943–948.

Przytulska A., Comte J., Crevecoeur S., Lovejoy C., Laution I., Vincent W.F. (2016) Phototrophic pigment diversity and picophytoplankton in permafrost thaw lakes. Biogeosciences 13, 13-26.

Rautio, M., Dufresne, F., Laurion, I., Bonilla, S., Vincent, W.F., Christoffersen, K.S., 2011. Shallow freshwater ecosystems of the circumpolar Arctic. Écoscience 18, 204–222. http://dx.doi.org/10.2980/18-3-3463.

Richardson, H., Waldron, S., Whitaker, J., Ostle, N., 2015. Measures of peatland carbon cycling from peat mesocosm incubation experiments. NERC Environmental Information Data Centre. http://dx.doi.org/10.5285/e15fbbab-1cdd-4509-81a3-aa050e927dd0.

Roehm, C.L., Giesler, R., Karlsson, J., 2009. Bioavailability of terrestrial organic carbon to lake bacteria: the case of a degrading high-latitude boreal and Arctic permafrost mire complex. J Geophys Res 114, Art No G03006.

Roiha, T., Rautio, M., Laurion, I., 2015. Carbon dynamics in highly net heterotrophic subarctic thaw ponds. Biogeosciences 12, 7223–7237. http://dx.doi.org/10.5194/bg-12-7223-2015.

Roiha, T., Peura, S., Cusson, M., Rautio, M., 2016. Allochthonous carbon is a major regulator of bacterial growth and community composition in subarctic freshwaters. Sci. Rep. 6: 34456, doi: 10.1038/srep34456.

Romanovsky, V.E., Smith, S.L., Christiansen, H.H., 2010. Permafrost thermal state in the polar Northern Hemisphere during the international polar year 2007–2009: a synthesis. Permafr. Periglac. Process. 21, 106–116. https://doi.org/10.1002/ppp.689

Schuur, E.A.G., McGuire, A.D., Schädel, C., Grosse, G., Harden, J.W., Hayes, D.J., Hugelius, G., Koven, C.D., Kuhry, P., Lawrence, D.M., Natali, S.M., Olefeldt, C., Romanovsky, V.E., Schaefer, K., Turetsky, M.R., Treat, C.C., Vonk. J.E., 2015. Climate change and the permafrost carbon feedback. Nature 520, 171–179. http://dx.doi.org/10.1038/nature14338.

Sepulveda-Jauregui, A., Walter Anthony, K. M., Martinez-Cruz, K., Greene, S. & Thalasso, F., 2015. Methane and carbon dioxide emissions from 40 lakes along a north–south latitudinal transect in Alaska. Biogeosciences 12, 3197–3223.

Serikova, S., Pokrovsky, O.S., Laudon, H., Krickov, I.V., Lim, A.G., Manasypov, R.M., Karlsson, J., 2019. High carbon emissions from thermokarst lakes of Western Siberia. Nature Communications, 10, Art No 1552. https://doi.org/10.1038/s41467-019-09592-1.

Shirokova, L.S., Pokrovsky, O.S., Kirpotin, S.N., Desmukh, C., Pokrovsky, B.G., Audry, S. Viers, J., 2013. Biogeochemistry of organic carbon, CO_2, CH_4, and trace elements in thermokarst water bodies in discontinuous permafrost zones of Western Siberia. Biogeochemistry 113, 573–593. http://dx.doi.org/10.1007/s10533-012-9790-4.

Shirokova, L.S., Kunhel, L., Rols, J.-L., Pokrovsky, O.S., 2015. Experimental modeling of cyanobacterial bloom in a thermokarst lake. Aquat. Geochem. 21, 487–511. http://dx.doi.org/10.1007/s10498-015-9269-8.

Shirokova, L.S., Bredoire, R., Rols, J.-L., Pokrovsky, O.S., 2017. Moss and peat leachate degradability by heterotrophic bacteria: The fate of organic carbon and trace metals. Geomicrobiol. J. 34(8), 641-655. http://dx.doi.org/10.1080/01490451.2015.1111470.

Shirokova, L.S., Chupakov, A.V., Zabelina, S.A., Neverova, N.V., Payandi-Rolland, D., Causserand, C., Karlsson, J., Pokrovsky, O.S., 2019. Humic surface waters of frozen peat bogs (permafrost zone) are highly resistant to bio- and photodegradation. Biogeosciences 16, 2511–2526. https://doi.org/10.5194/bg-16-2511-2019.

Shirokova, L.S., Payandi-Rolland, D., Lim, A., Manasypov, R.M., Allen, J., Bénézeth P., Rols, J.-L., Karlsson, J., Pokrovsky, O.S., 2020. Diurnal cycle of C concentration and emission fluxes in humic thaw ponds of frozen peatlands: application for C balance constraints. Sci. Total Environ. 737, Art No 139671, https://doi.org/10.1016/j.scitotenv.2020.139671

Squires, M.M., Lesack, L.F.W., Hecky, R.E., Guilford, S.J., Ramlal, P., Higgins, S.N., 2009. Primary production and carbon dioxide metabolic balance of a lake-rich Arctic river floodplain: Partitioning of phytoplankton, epipelon, macrophyte, and epiphyton production among lakes on the Mackenzie Delta. Ecosystems 12, 853-872, doi: 10.1007/s10021-009-9263-3.

Stutter, M.I., Richards, S., Dawson, J.J.C., 2013. Biodegradability of natural dissolved organic matter collected from a UK moorland stream. Water Res. 47(3), 1169-1180.

Tank, S.E., Lesack, L.F.W., Hesslein, R.H., 2009. Northern delta lakes as summertime CO_2 absorbers within the Arctic landscape. Ecosystems 12, 144-157, doi: 10.1007/s10021-008-9213-5.

Voigt, C., Marushchak, M.E., Mastepanov, M., Lamprecht, R.E., Christensen, T.R…. Biasi C., 2019. Ecosystem carbon response of an Arctic peatland to simulated permafrost thaw. Global Change Biology 25, 1746-1764, doi: 10.1111/gcb.14574.

Vonk, J.E., Tank, S.E., Bowden, W.B. Laurion, I., Vincent, W.F., Alekseychik, P., Amyot, M., Billet, M.F., Canário, J., Cory, R.M., Deshpande, B.N., Helbig, M., Jammet, M., Karlsson, J., Larouche, J., MacMillan, G., Rautio, M., Walter Anthony, K.M., Wickland, K.P., 2015. Reviews and syntheses: Effects of permafrost thaw on Arctic aquatic ecosystems. Biogeosciences 12, 7129–7167. http://dx.doi.org/10.5194/bg-12-7129-2015.

Walter, K.M., Chanton, J.P., Chapin III, F.S., Schuur, E.A.G., Zimov, S.A., 2008. Methane production and bubble emissions from arctic lakes: Isotopic implications for source pathways and ages. J. Geophys. Res. 113, G00A08. http://dx.doi.org/10.1029/2007JG000569.

Walter Anthony, K.M., Anthony, P., Grosse, G., Chanton, J., 2012. Geologic methane

seeps along boundaries of Arctic permafrost thaw and melting glaciers. Nature Geosci. 5, 419–426. http://dx.doi.org/10.1038/ngeo1480.

Walter Anthony, K.M., Zimov, S.A., Grosse, G., Jones, M.C., Anthony, P.M., Chapin III, F.S., Finlay, J.C., Mack, M.C., Davydov, S., Frenzel, P., Frolking, S., 2014. A shift of thermokarst lakes from carbon sources to sinks during the Holocene epoch. Nature 511, 452–456. http://dx.doi.org/10.1038/nature13560.

Wauthy, M., Rautio, M., Christoffersen, K.S., Forsström, L., Laurion, I., Mariash, H., Peura, S., Warwick, V.F., 2018. Increasing dominance of terrigenous organic matter in circumpolar freshwaters due to permafrost thaw. Limnol. Oceanogr. Letters 3 (3), 186-198, DOI : 10.1002/lol2.10063

Wauthy M., Rautio M., 2020. Permafrost thaw stimulates primary producers but has a moderate effect on primary consumers in subarctic ponds. Ecosphere 11(6), Article e03099.

Wik, M., Varner, R.K., Anthony, K.W., MacIntyre, S., Bastviken, D., 2016. Climate-sensitive northern lakes and ponds are critical components of methane release. Nature Geosci. 9, 99–105. http://dx.doi.org/10.1038/ngeo2578.

Zabelina, S.V., Shirokova, L.S., Klimov, S.I., Chupakov, A.V., Lim, A.G., et al., 2021. Seasonal and spatial variations of CO_2 and CH_4 concentrations and fluxes in surface waters of frozen peatlands (NE Europe): morphological and hydrochemical control. Limnology Oceanography 66 (S1), S216-S230. doi: 10.1002/lno.11560.

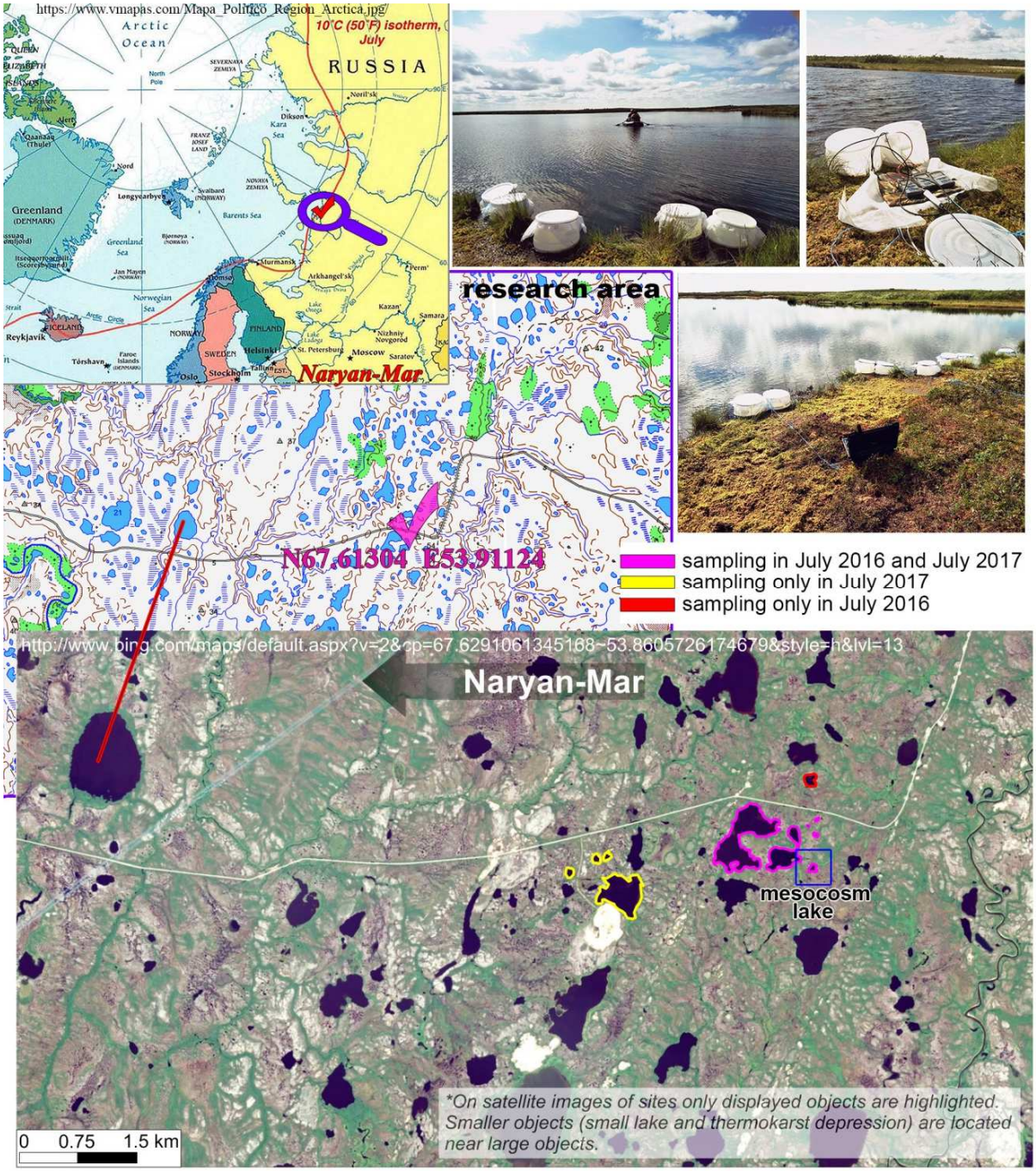

Figure 1 A: The map of the study site with position of sampled lakes and photos of mesocosm run at the lake shore.

1018

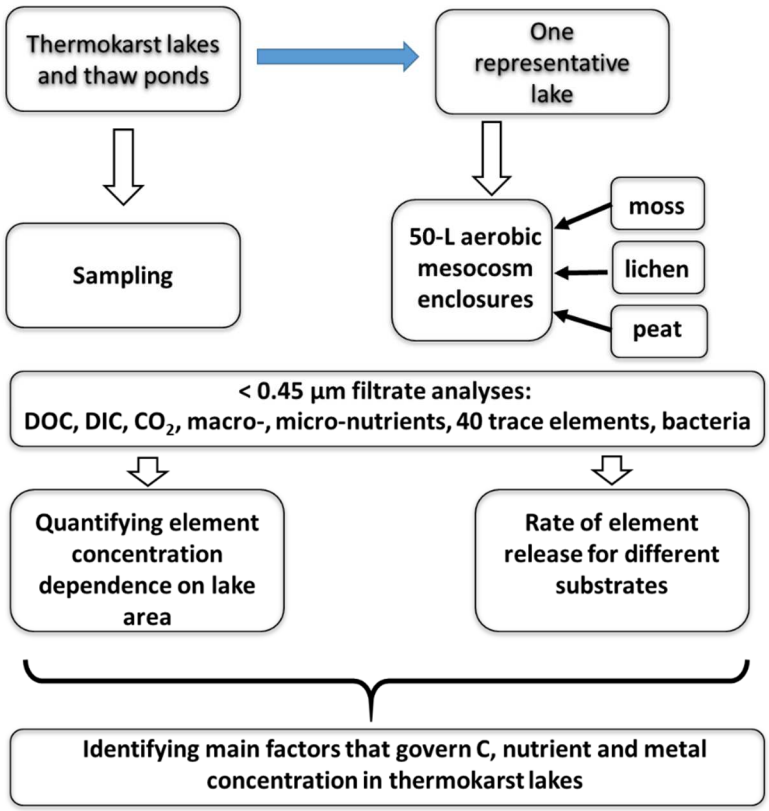

1019

1020

1021 **Figure 1 B:** The work flow chart of the field observations, mesocosm experiments and
1022 analyses performed in this study.

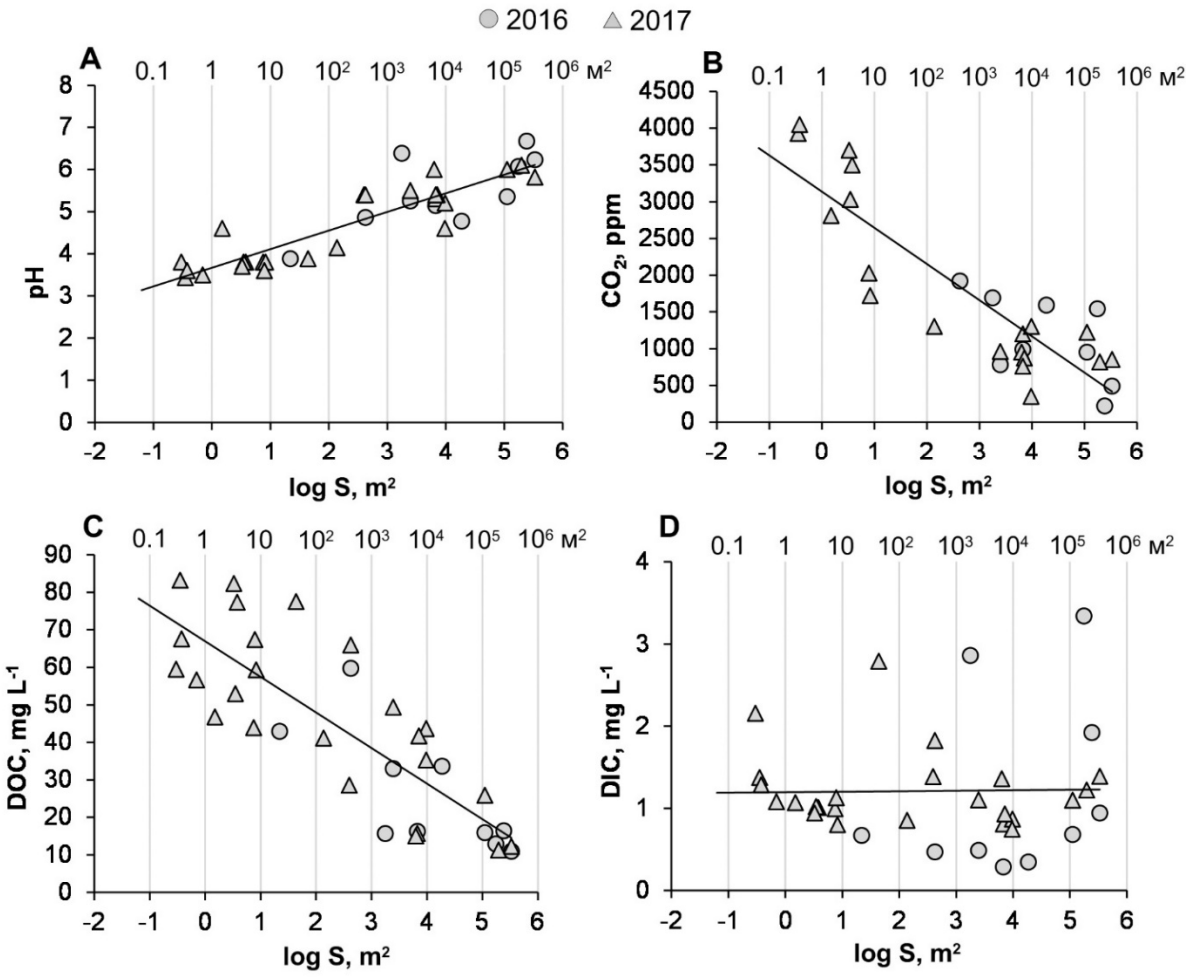

Figure 2. pH (A), pCO2 (B), DOC (C) and DIC (D) concentration in depressions, thaw ponds and thermokarst lakes as a function of logarithm of lake surface area (log S). Parameters of linear relationships (Eqn. 1) are listed in Table S1 of the Supplement.

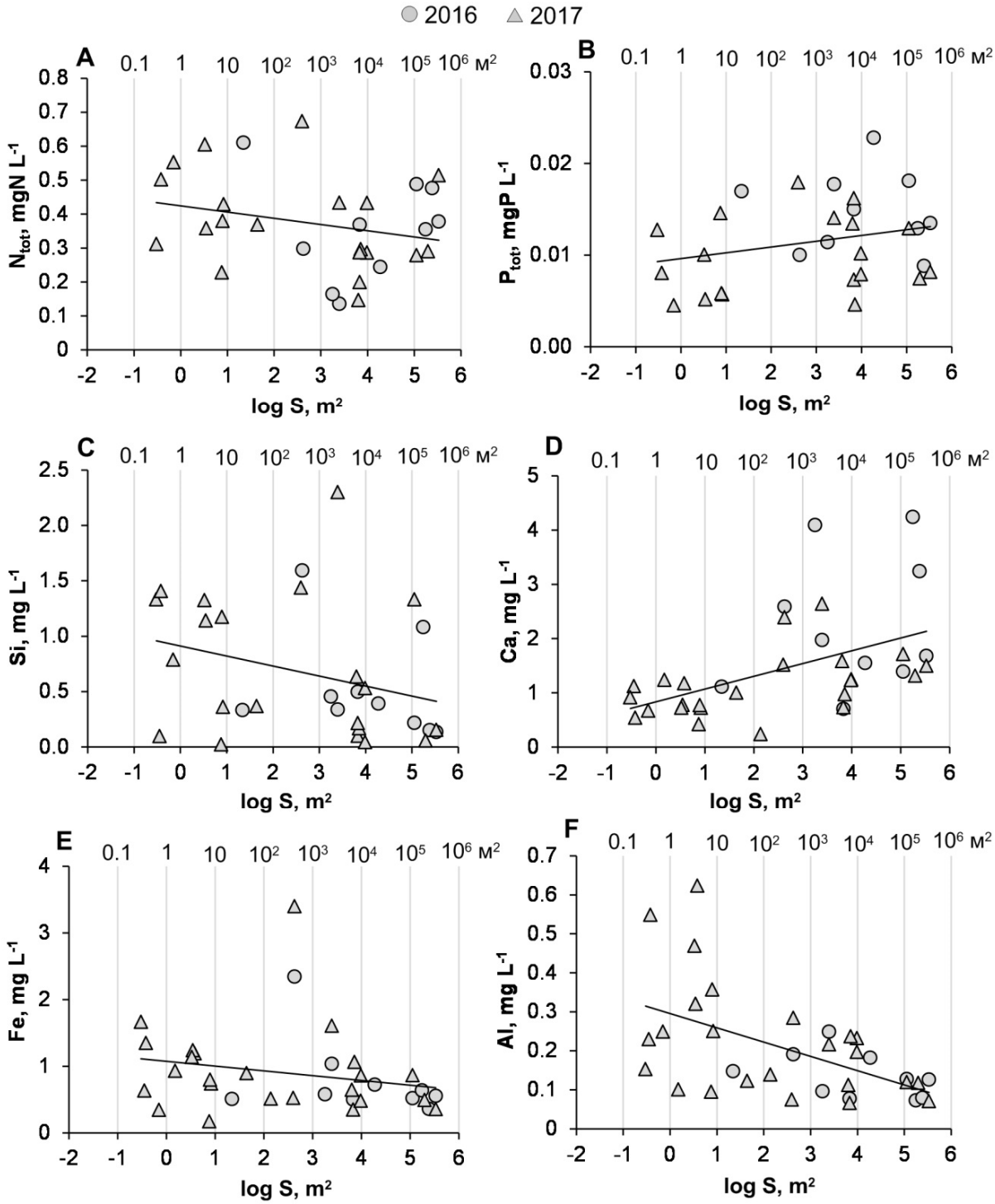

1038

1039

1040 **Figure 3.** Total dissolved N (A), P (B), Si (C), Ca (D), Fe (E) and Al (F) concentrations
1041 in depressions, thaw ponds and thermokarst lakes as a function of logarithm of
1042 lake surface area (log S). Parameters of linear relationships are listed in Table S1.

1043

1044

1045

1046

1047

1048

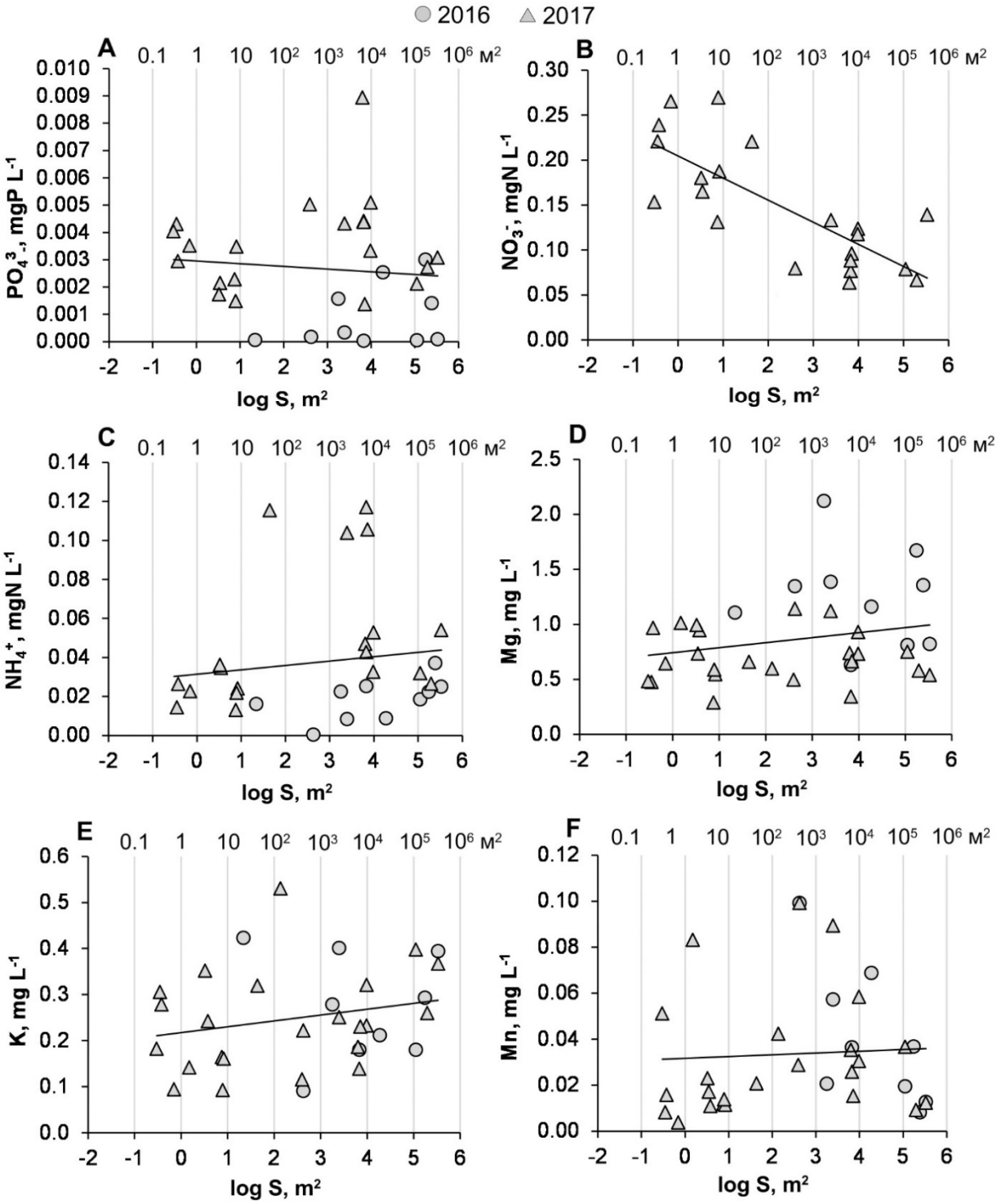

Figure 3, continued. Phosphate, nitrate, ammonia, Mg, K and Mn concentrations in thermokarst water bodies as a function of logarithm of lake surface area (log S).

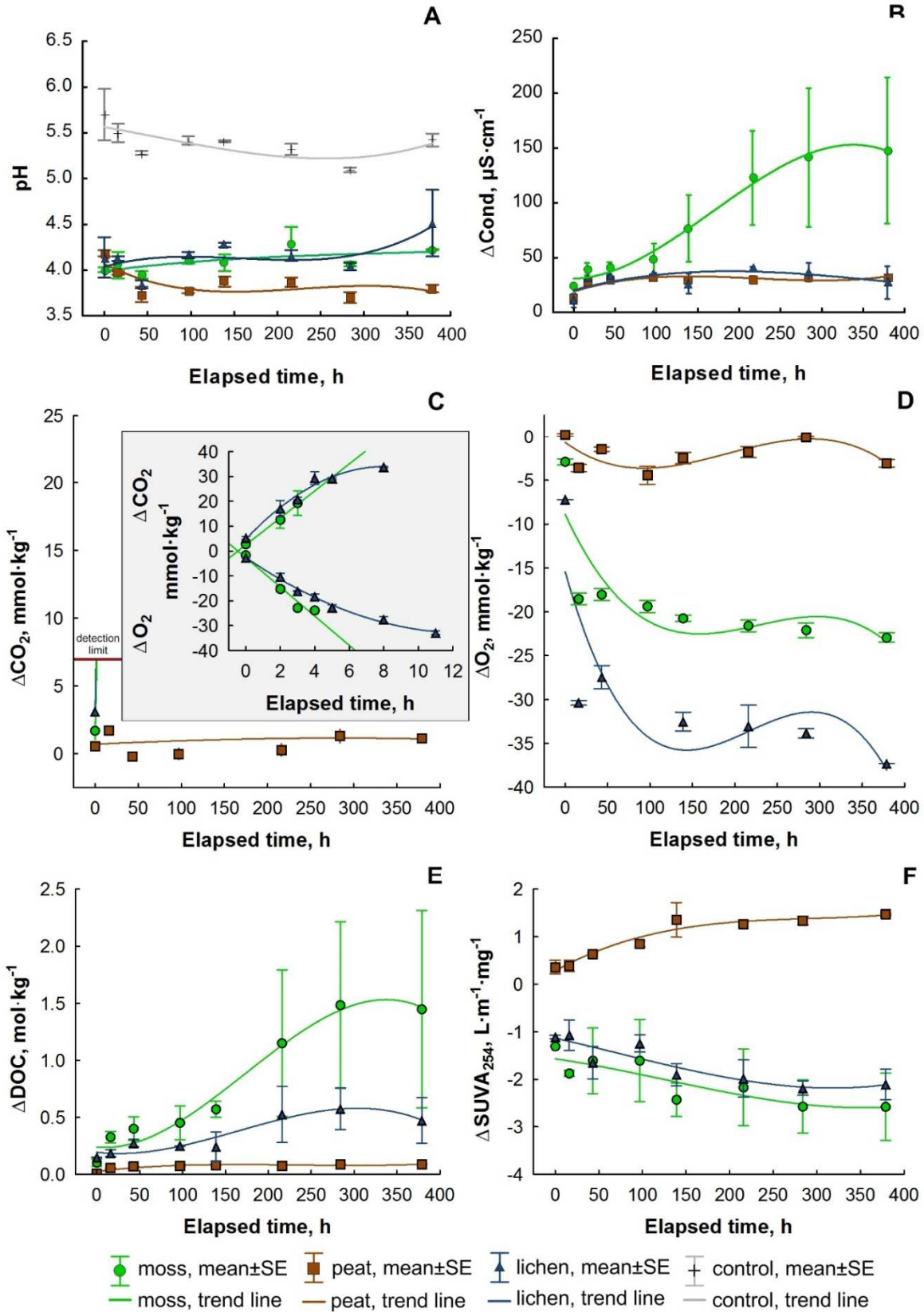

Figure 4. The pH value (**A**), and the difference between experiment (moss, lichen or peat) and control (lake water without substrate) in Specific Conductivity (**B**), O_2 (**C**), pCO_2 (**D**), DOC (**E**) concentrations and $SUVA_{254}$ (**F**) in mesocosms as a function of exposure time. Here and in other figures below, symbols represent the mean; the error bars correspond to the S.E. of two independent duplicate experiments. Solid lines represent a polynomial fit to the data that was used to calculate the maximal rates and concentration yields.

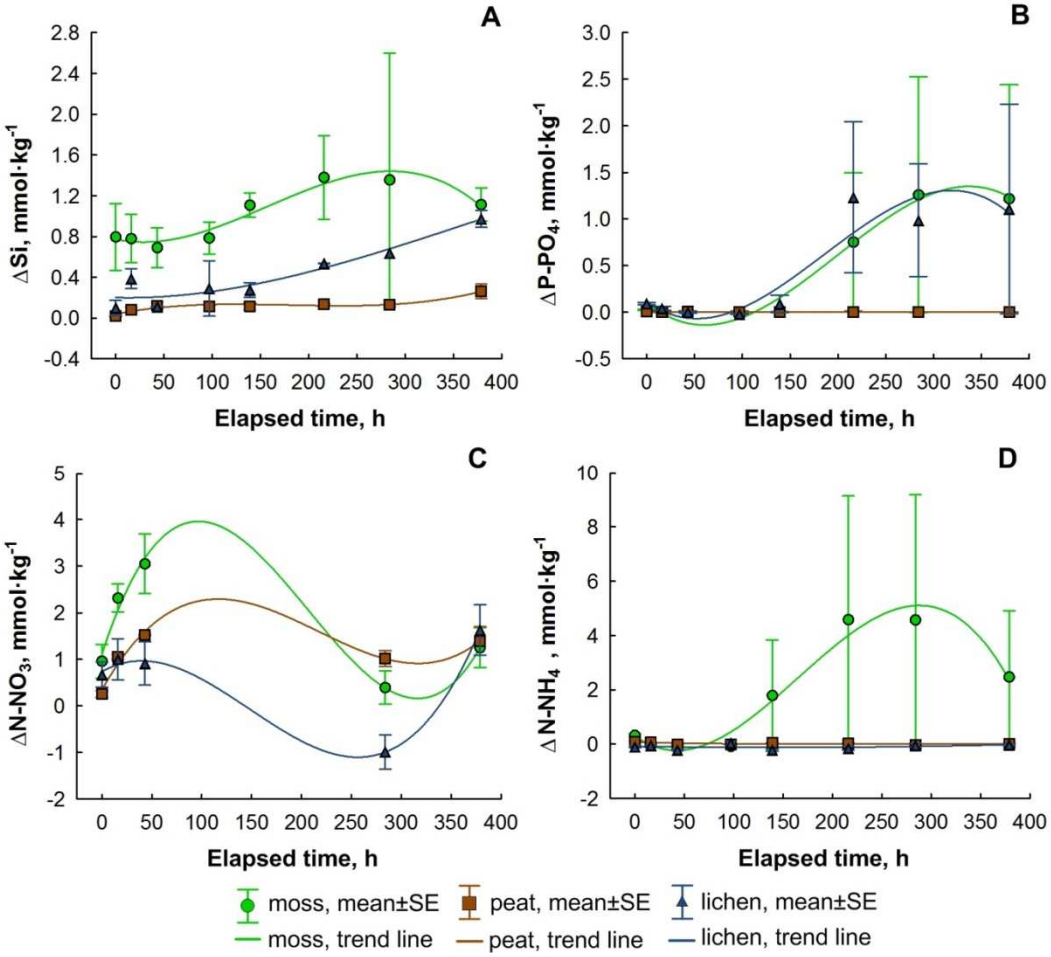

Figure 5. Evolution of the difference in Si (A), PO_4 (B), NO_3 (C), and NH_4 (D) concentrations between the mesocosm (moss, lichen or peat) and control in the course of experiments. See Fig. 4 caption for detailed legend.

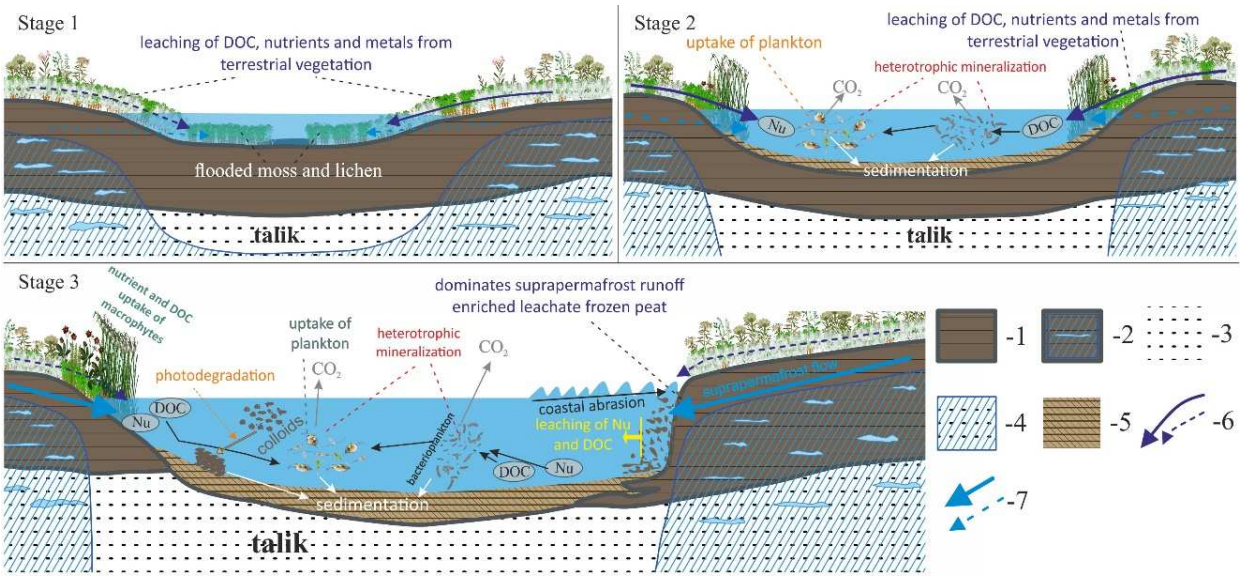

Legend:
1 - Peat of active (unfrozen) layer
2 - Frozen peat with ice lenses
3 - Unfrozen mineral horizons
4 - Frozen mineral horizons
5 - Lake sediments
6 - Flux of DOC and nutrients that are leached from plant litter
7 - Flux of DOC and nutrients that are leached from peat (both active and permafrost layer)

Figure 6. A cartoon of thaw pond and thermokarst lake evolution and the change of sources of DOC and nutrients in the course of evolution, from surface moss and lichen to frozen peat. A three main stage sequence of thermokarst lake formation and development includes:
(1) soil depression filled by water which interacted with submerged moss and lichens thus leaching DOM and solutes to the lake;
(2) beginning of in-lake processing of DOM via heterotrophic plankton mineralization and sedimentation to the bottom, occurring under the dominance of allochthonous input from vegetation leaching;
(3) stage of large mature lake, influenced by nutrients and DOM input from thawed and frozen peat leaching and nutrients and CO_2 uptake by phytoplankton, under on-going DOM, nutrient and metal processing via photo- and biodegradation in the water column.

Table 1. The mean and maximal release rates and maximal concentration yield of major components normalized to dry weight of substrate in mesocosm experiments. Significant ($p < 0.05$) results are labelled with asterisk (*).

Index	Substr.	R^2	F-test (p=0.05)	υ_{mean}±SE, X·hr^{-1}	υ_{max}±SE, X·hr^{-1}	ΔC_{max}±SE	$T_{\Delta Cmax}$
EB, CFU·10^6·kg^{-1}	moss	0.64	7.2*	0.05±0.02	0.1±0.4	21±7	379
	peat	0.74	11.3*	0.022±0.001	0.036±0.004	2.1±0.1	97
	lichen	0.88	29.2*	0.00074±0.00001	0.33±0.03	58±3	379
OB, CFU·10^6·kg^{-1}	moss	0.92	48.3*	0.044±0.002	0.08±0.02	17.5±0.8	379
	peat	0.49	3.8*	0.012±0.005	0.05±0.02	5±1	216
	lichen	0.92	45.0*	0.11±0.02	0.23±0.09	42±6	379
O_2, mmol·kg^{-1} (long)	moss	0.68	8.62*	-0.128±0.007	-0.98±0.09	-22.9±0.7	379
	peat	0.52	4.3*	-0.05±0.01	-0.24±0.04	-4±1	97
	lichen	0.68	8.62*	-0.182±0.008	-1.45±0.02	-37	97
CO_2, mmol·kg^{-1} (short, for peat long)	moss	0.78	14.4*	6±2	6±2	19±5	3
	peat	0.10	0.44	0.0026±0.0007	-0.112±0.0064	4.7±0.7	139
	lichen	0.95	80.5*	4.23±0.04	6.0±0.8	33.8±0.4	8
DIC, mmol·kg^{-1}	moss	0.31	1.78	0.14±0.03	0.7±0.2	14±3	97
	peat	0.38	2.42	0.006±0.006	0.01±0.02	1±1	216
	lichen	0.90	37.7*	0.323±0.007	0.54±0.06	31.4±0.7	97
DOC, mmol·kg^{-1}	moss	0.52	4.39*	5±4	8±13	1484±1034	284
	peat	0.78	14.0*	0.52±0.05	1.5±0.1	89±2	284
	lichen	0.50	4.01*	2±1	4±5	577±184	284
NH_4^+, mmol(N)·kg^{-1}	moss	0.34	2.08	0.02±0.03	0.04±0.12	5±6	216
	peat	0.36	2.25	-0.0002±0.0001	0.0006±0.0005	-0.04±0.02	284
	lichen	0.11	0.49	0.0002±0.0002	0.0002±0.0010	0.03±0.08	97
NO_3^-, mmol(N)·kg^{-1}	moss	0.81	8.58*	0.05±0.03	0.08±0.06	3.1±0.9	43
	peat	0.85	11.1*	0.030±0.002	0.050±0.008	1.53±0.02	43
	lichen	0.80	8.18*	0.01±0.02	0.02±0.04	1.6±0.5	379
NO_2^-, µmol(N)·kg^{-1}	moss	0.70	9.44*	0.4±0.6	1±2	15±10	43
	peat	0.81	17.5*	0.05±0.02	0.10±0.06	9.8±0.5	379
	lichen	0.09	0.4	0.04±0.06	0.1±0.2	-21±2	16
N_{tot}, mmol(N)·kg^{-1}	moss	0.76	6.3*	0.014±0.009	0.04±0.03	8±2	284
	peat	0.88	14.3*	0.006±0.003	0.04±0.01	3.4±0.5	379
	lichen	0.75	6.09*	0.03±0.01	0.09±0.08	12±4	379
PO_4^{3-}, µmol(P)·kg^{-1}	moss	0.38	2.46	4±6	7±42	1262±1790	284
	peat	0.04	0.16	-0.016±0.007	0.01±0.14	0.7±0.4	139
	lichen	0.43	3.03	5±4	11±7	1234±812	216
P_{tot}, µmol(P)·kg^{-1}	moss	0.47	1.79	0.4±0.2	0.7±0.3	1647±2146	379
	peat	0.19	0.45	-0.02±0.20	0.27±0.05	54±32	0
	lichen	0.54	2.32	5±4	7±5	1695±1068	284
Si, mmol·kg^{-1}	moss	0.20	0.99	0.003±0.005	0.005±0.007	1.4±0.6	216
	peat	0.75	11.8*	0.0007±0.0003	0.0024±0.0009	0.26±0.07	379

	lichen	0.76	12.76*	0.0023±0.0004	0.0035±0.0009	0.97±0.08	379
	moss	0.80	15.8*	0.08±0.04	0.11±0.1	32±16	379
Na, mmol·kg^{-1}	peat	0.69	8.98*	0.0005±0.0002	0.0036±0.0005	-0.035±0.005	379
	lichen	0.63	6.67*	0.03±0.02	0.06±0.02	9±1	284
	moss	0.62	6.53*	0.2±0.2	0.3±0.4	70±49	379
K, mmol·kg^{-1}	peat	0.13	0.6	0.00002±0.00020	-0.0014±0.0004	-0.03±0.05	379
	lichen	0.34	2.05	0.185±0.005	0.37±0.02	22.5±0.1	97
	moss	0.24	1.27	0.01±0.01	0.01±0.03	3±3	284
Ca, mmol·kg^{-1}	peat	0.68	8.55*	0.008±0.002	0.019±0.008	0.7±0.2	379
	lichen	0.85	22.5*	-0.015±0.001	-0.03±0.01	-2.21±0.01	139
	moss	0.34	2.04	0.02±0.02	0.02±0.05	5±7	379
Mg, mmol·kg^{-1}	peat	0.81	17.2*	0.0005±0.0001	0.002±0.001	-0.45±0.02	379
	lichen	0.82	18.2*	-0.025±0.003	-0.10±0.02	-1.6±0.1	97
	moss	0.48	3.69*	0.0014±0.0005	0.003±0.003	0.14±0.03	97
Al, mmol·kg^{-1}	peat	0.91	39.3*	0.00041±0.00003	0.0018±0.0003	0.149±0.007	379
	lichen	0.99	263*	-0.0014±0.0002	-0.0028±0.0007	-0.223±0.006	379
	moss	0.54	4.63*	0.004±0.002	0.005±0.006	1.4±0.4	284
Fe, mmol·kg^{-1}	peat	0.91	42.3*	0.00040±0.00004	0.0007±0.0004	0.086±0.009	379
	lichen	0.85	22.2*	-0.0054±0.0001	-0.0167±0.0005	-0.959±0.007	97

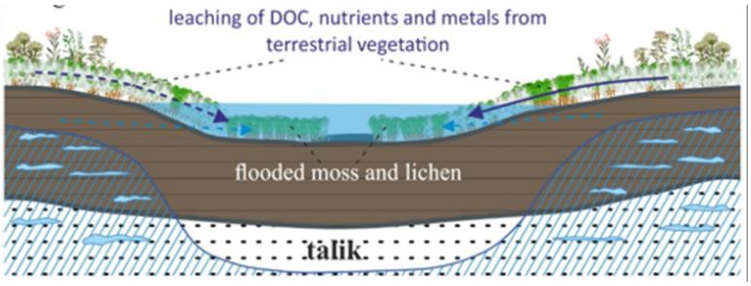

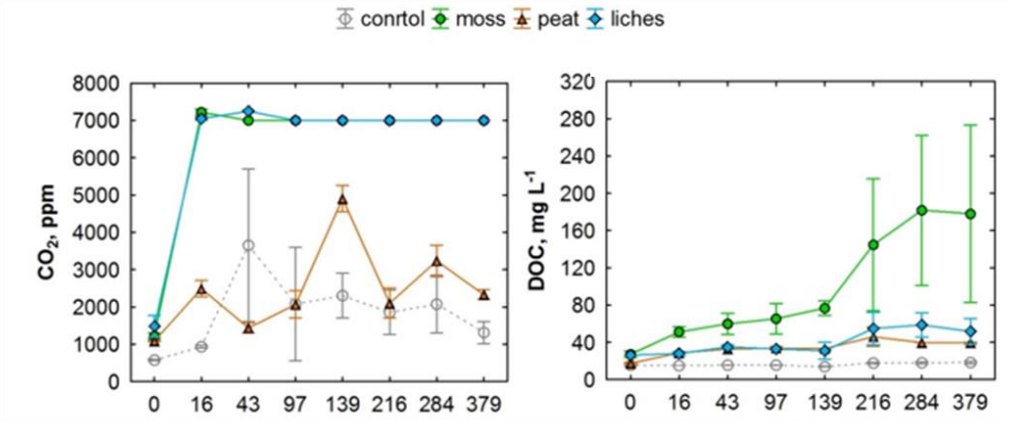

Elapsed time in mesocosm, hr